

Unpacking the Eye of the Beholder: Social Location, Identity, and the Moving Target of Political Perspectives*

Elena Sirotkina
Center for Data Science
New York University
es7093@nyu.edu

May 2026

Abstract

Political and social identities structure how people evaluate political information, a finding decades deep in political science and routinely discarded by computational tools that often produce single scores that treat a piece of text, an image, or a video as if it means the same thing to everyone. This paper shows that it does not, and that the difference is consequential. To address this problem, I develop the Perspectivist Visual Political Sentiment (PVPS) classifier, which learns from approximately 82,000 evaluations by 5,575 U.S. adults to predict how audiences defined by political and social identities will evaluate the same image. Unlike standard tools that average systematic disagreement away, PVPS preserves it, returning an evaluative profile that records who agrees, who diverges, and along which identity lines. Applied to several influential studies of visual sentiment, PVPS shows that perceived violence in protest imagery and the emotional mechanisms behind protest image engagement both change substantively once audience identity is taken into account. It follows that what a political image conveys is a moving target, and measuring it requires knowing whom it is moving.

*I am grateful to Andreu Casas, Nora Webb Williams, Alex Todorov, and Donghyeon Won for sharing their datasets with me. All errors are my own.

Introduction

The rise of machine learning has given political science a new empirical frontier. Text, images, audio, and video, the media through which political life is increasingly conducted, can now be classified and analyzed at scale, largely drawing on tools from computer vision and NLP that were simply out of reach a decade ago (Barberá et al., 2015; Grimmer and Stewart, 2013; Joo and Steinert-Threlkeld, 2022; Lucas et al., 2015).

But adoption comes with a price. These tools were built for tasks where a correct answer exists independently of the observer, so the entire infrastructure assumes that disagreement is error to be eliminated. Applied to evaluative tasks - and political sentiment is evaluative at its core - the model learns to predict whichever label the annotator pool produced, performing well by every standard metric, while what was averaged away was the phenomenon political science actually cares about. These are the lines of tension and evaluative conflict that define political disagreement in the first place.

The Perspectivist Visual Political Sentiment (PVPS) classifier developed here is built around this disagreement. Instead of predicting a single sentiment score, it produces an evaluative profile for each image that records which audiences rate it more favorably, along which social and political fault lines, and with what confidence. The classifier is trained on approximately 82,000 ratings of 1,264 political images from 5,575 U.S. adults with full demographic batteries (four survey waves, 2022–2025) and validated against a separate corpus of 7,543 images annotated by over 2,000 workers, drawing on a combined pool of roughly 8,800 unique images and 7,700 respondents.

From this, the classifier learns which visual features of an image predict evaluative divergence between groups, and it applies that learning to images it has never seen. This architecture answers the question that political science actually asks about political images, that where a person stands, politically and socially, determines what they see in a political visual (see e.g. Torres, 2021; Webb Williams, Casas, and Wilkerson, 2020), and the classifier makes that structured variation measurable and predictable at scale.

I use PVPS for Casas and Webb Williams's (2019) finding that enthusiasm mobilizes sharing of Black Lives Matter images. The emotional mechanisms hold, but they operate differently depending on which partisan-demographic group the image favors. On the Democratic Women vs. Republican Men axis, enthusiasm produces a steeper mobilization slope for Democrat-women-favorable images, while fear and disgust generate sharply higher engagement for Republican-men-favorable ones. Images that received higher perceived violence scores in Won, Steinert-Threlkeld, and Joo's (2017) annotation scheme are the same images that the classifier predicts as more favorably evaluated by Republican, conservative, and Republican-leaning respondents.

The contribution of this study runs in both directions across the disciplinary boundary. For political science, the discipline has long established that political evaluation is group-mediated (Campbell et al., 1960), identity-sorted (Mason, 2018), and intersectional rather than additive (Crenshaw, 1991; Hancock, 2007), and yet the empirical tools available have not kept pace with the theory. Surveys aggregate evaluation across groups but human annotation collapses disagreement into a majority label, which loses group-specific predicted reactions across multiple social tension dimensions simultaneously. Here I propose an approach that makes group-mediated evaluation measurable at scale and applicable to corpora that survey methods reach more rarely.

For computational political science, the field has documented the construct-validity risks that arise when tools built for objective tasks are applied to evaluative ones (Bestvater and Monroe, 2023; Gasparyan and Sirotkina, 2024; Grimmer, Roberts, et al., 2022). PVPS shows that the axes of group conflict over political images carry a signal strong enough to be modeled directly from visual content. Once this signal is incorporated into the analysis, the interpretation of how images are received changes substantially. This makes it possible to reanalyze media and visual persuasion effects at scale and re-examine their long-term influence across millions of observations.

Disagreeing Perspectives in Politics

Politics is essentially about disagreement. Classic work in political science and sociology treats political conflict as the mobilization of social difference (Mouffe, 2005; Schattschneider, 1960; Schmitt, 2007), which have crystallized into political divisions that outlast the conflicts producing them (Bartolini and Mair, 1990; Flora et al., 1999; Hooghe et al., 2002; Kriesi et al., 2008; Lipset and Rokkan, 1967).

These structural divisions are lived through social location, conceived as the core of a person's existence in the social and political world (Berger and Luckmann, 1966; Mannheim, 1936), which underlies *perspectival* disagreement as an unavoidable condition of human social interaction (Kinder and Kam, 2009; Mason, 2018). As people learn early which social and political groups they belong to (Campbell et al., 1960; Converse, 1964), these attachments operate as perceptual filters throughout life (Campbell et al., 1960; Jennings and Niemi, 1981). The tighter a person's group attachment, the more coherent their political orientations tend to be (Tajfel and Turner, 1979).

Political science has devoted extensive attention to how social location—e.g., race (Jardina, 2019) and ethnicity (Kinder and Kam, 2009), gender (Dugger, 1988; Phoenix, 2019), class (Wright, 1997), and their intersections (Crenshaw, 1991) - shapes political judgment through group-based heuristics and intuition (Achen and Bartels, 2016; Haidt, 2012; Mason, 2018). Family, education, and discussion networks reinforce this coherence (Achen and Bartels, 2016; Huckfeldt and Sprague, 1995) by strengthening the link between group identity and judgment. In other words, where you stand determines what you see, and what you see determines how you judge (Campbell et al., 1960; Kahan, 2013; Kinder and Kam, 2009).

Understanding political disagreement, in this tradition, requires understanding the social structure that produces it. But this also implies that if political evaluation is structured by identity and social location, then any attempt to measure it inherits this structure. This is where the rise of computational social science creates both opportunity and risk.

Computational tools are increasingly used to measure and predict political attitudes¹ at scale and these are tasks that depend on human-generated labels and therefore on the same dynamics political science has long studied. Yet these tools have largely developed without integrating what political science and sociology already know about the *anticipated* lines of social and political disagreement. The following sections examine how social location and predictive computation intersect, what current approaches miss, and how a perspectivist framework advanced here can address the gap.

The Moving Target of 'Ground Truth' in Computation

Making of the "Ground Truth"

Computational approaches to text, image, and multimodal classification have long operated under a paradigm of ground truth absolutism, wherein the goal of annotation is to converge on a single correct label that represents the "true" state of each data instance (Cabitza et al., 2023; Frenda et al., 2025; Uma et al., 2021).

This assumption is built into supervised machine learning itself. Classifiers learn to map inputs to outputs, which means they typically need a single correct answer for each example to measure how well they are doing (Uma et al., 2021). But when multiple people label the same piece of text, they can disagree. Standard training procedures cannot handle multiple answers at once,² so majority voting became the default solution, picking whichever label got the most votes (Cabitza et al., 2023; Mostafazadeh Davani et al., 2022). The resulting infrastructure was designed to collect redundant labels only to col-

¹Or any attitudinal outcome that approximates political attitudes, including sentiment, perceptions, and related evaluative responses.

²A model learns by guessing an answer and measuring how wrong it was. The standard formula (cross-entropy with a one-hot target) expects one correct answer per example, but replacing the one-hot vector with the empirical distribution of annotator responses is a one-line change that existing frameworks support natively (Peterson et al., 2019). Majority voting became the default not because alternatives are technically infeasible but because annotation platforms were built around single-label output and most pipelines inherited that convention (Cabitza et al., 2023).

lapse them and treating disagreement as "noise" (Aroyo and Welty, 2015; Dumitrache et al., 2018).

In other words, this "gold standard" framing carried implicit epistemic commitments that categories are ontologically discrete, that competent annotators should agree, and that residual disagreement indicates either task ambiguity requiring clearer guidelines or annotator unreliability requiring filtering (Raykar et al., 2010; Russell et al., 2008).

But as more recent and subsequent work would reveal, this convenience came at the cost of erasing exactly the human variation that matters most for subjective tasks (see e.g. Fornaciari et al., 2021; Pavlick and Kwiatkowski, 2019; Röttger et al., 2022).

AI fairness, for example, has demonstrated that training data is never neutral because when it reflects one group's judgments disproportionately, the resulting model reproduces those judgments as default (Barocas and Selbst, 2016; Mehrabi et al., 2021). Applied to annotation, this means that a single-label approach does not approximate a universal ground truth but privileges whoever is most represented in the annotator pool (Plank, 2022; Prabhakaran et al., 2021).

Together, these findings raise fundamental concerns about the validity of using aggregated labels as the default approach to training predictive models. When evaluation is shaped by social position, aggregation does not approximate truth but it privileges whoever is most represented in the data.

Whose Ground is More Truth? Perspectivism as a Framework for Computational Political Science

At the same time, the boundary between tasks where a single ground truth is appropriate and tasks where it is not remains poorly defined. Whenever a task engages political or social identity, annotators bring perspectives shaped by who they are. Yet disagreement surfaces even on supposedly objective tasks like part-of-speech tagging (Plank, 2022) or medical diagnosis (Cabitza et al., 2023), suggesting that ground truth is less stable than

assumed. Table 1 summarizes the five most frequently cited sources of such disagreement.

In political science, trained coders exhibit systematic disagreement that propagates into position estimates (Benoit et al., 2016; Mikhaylov et al., 2012). Partisans assign divergent labels to identical images (Gasparyan and Sirotkina, 2025; Webb Williams, Casas, Aslett, et al., 2026), annotator characteristics shape hate speech judgments (Sap, Card, et al., 2019; Waseem, 2016), toxicity ratings (Goyal et al., 2022; Prabhakaran et al., 2021; Sap, Swayamdipta, et al., 2022), and much of the subjective content broadly defined (Mostafazadeh Davani et al., 2022).

A growing body of work treats this disagreement as signal rather than noise, a position formalized as **perspectivism** (Cabitza et al., 2023). Rather than collapsing annotations into a single label, perspectivism retains who rated each item and what attributes they carry. Table 2 compares the two levels Cabitza et al. (2023) distinguish. Weak perspectivism acknowledges that annotators differ and may weight their contributions unequally, but still produces a single aggregated label. Strong perspectivism abandons aggregation and preserves the full distribution of annotations and treats it as the object of interest.

Yet existing perspectivist work³ largely reduces disagreement to a single demographic or social dimension, despite perspectivism being fundamentally concerned with heterogeneous and intersecting evaluations. For example, prior work on textual analysis conditions only on race in toxicity detection (Sap, Card, et al., 2019; Sap, Swayamdipta, et al., 2022) or demographic groups in hate speech (Fleisig et al., 2023). In other words, most perspectivist datasets record attributes in isolation rather than as overlapping identity structures (Orlikowski et al., 2023). This is also limiting for political judgment, which emerges at the intersection of political and social identity.

³Many works do not appear under the perspectivist label, but they effectively implement the same idea.

Table 1: Taxonomy of Annotator Disagreement[†]

Source	Characteristics	Resolution
<i>Resolvable disagreement (reducible through improved design)</i>		
1. Category overlap (Aroyo and Welty, 2015)	Overlapping or ambiguous categories force artificial discretization onto continuous reality, producing systematic label confusion	Improve taxonomy and annotation guidelines
2. Stimulus quality (Schaeckermann et al., 2018)	Degraded, incomplete, or insufficient stimuli prevent annotators from forming a confident judgment	Improve data quality; filter ambiguous stimuli
3. Task design (Xu and Jurgens, 2026)	Guidelines, interface, and response format constrain what annotators can express	Redesign annotation protocol
4. Reliability variation (Raykar et al., 2010)	Annotators differ in competence on tasks with a verifiable correct answer (e.g., named entity recognition, bill passage)	Weight by estimated accuracy; aggregate to single label
<i>Irreducible disagreement (structured by annotator identity)</i>		
5. Identity-structured evaluation (Gasparyan and Sirotkina, 2025; Prabhakaran et al., 2021; Sap, Card, et al., 2019; Sap, Swayamdipta, et al., 2022)	Disagreement is systematic by social location (partisanship, race, gender); reflects genuine evaluative differences rather than error	Strong perspectivism (model full annotation distribution; condition predictions on annotator characteristics)

[†]The boundary between resolvable and irreducible disagreement is a continuum, not a clean partition. In practice, many annotation instances contain both types simultaneously (Plank, 2022; Schaeckermann et al., 2018). The categories above are analytic distinctions that help guide methodological choices, not ontological claims about the nature of any specific disagreement.

Table 2: Weak vs. Strong Perspectivism[‡]

	Weak Perspectivism	Strong Perspectivism
1. Epistemological assumption	A correct answer exists; some annotators approximate it better	Multiple valid answers coexist; correctness is group-relative
2. Prediction target	Single aggregated label	Distribution over labels or per-group predictions
3. Disagreement is treated as	Noise to reduce	Signal to model
4. Typical methods	Reliability weighting, Dawid-Skene, item-response models (Raykar et al., 2010; Uma et al., 2021)	Multi-task heads, soft-label training (Fornaciari et al., 2021; Mostafazadeh Davani et al., 2022)
5. Appropriate for	Factual coding tasks (entity recognition, event detection, bill status)	Evaluative tasks (sentiment, tone, framing, toxicity)
6. Risk if misapplied where the <i>other</i> approach is warranted	Compresses legitimate disagreement into a single number; privileges whichever group dominates the annotator pool	Adds unnecessary complexity to factual tasks; may model noise as if it were perspective
7. Empirical evidence	Standard in supervised NLP; well-validated for factual annotation	Models trained on disaggregated labels match or outperform majority-vote baselines when evaluated against human distributions (Fornaciari et al., 2021; Pavlick and Kwiatkowski, 2019; Uma et al., 2021)

[‡]The distinction between weak and strong perspectivism was introduced by Cabitza et al. (2023). Strong perspectivism does not deny that ground truth exists for factual tasks; it holds that for evaluative tasks the annotation distribution *is* the phenomenon of interest, and collapsing it discards exactly the variation that matters.

This paper therefore introduces two contributions: (1) it brings perspectivism from text into the visual domain in political science by building a classifier that conditions predicted sentiment on audience identity rather than treating it as a fixed property of the image, and (2) it moves beyond single-axis conditioning by modeling multiple dimensions of social location simultaneously and showing that which dimension drives evaluative divergence varies across images. Both follow from the premise that political judgment is not independent of the judge. And therefore, identity-triggering evaluations are unavoidably filtered through the group identities they carry, which shape the interpretive frames they bring to any given political image.⁴

Perspectivist Visual Political Sentiment (PVPS)

This shift from content-centered prediction to audience-conditioned evaluation requires extending computer vision beyond detecting visual content only. Computer vision has made remarkable progress in political science for tasks where the goal is to identify what is in an image and how it is politically relevant, including protest framing (Torres, 2021; Won et al., 2017), face recognition (Joo, Steen, et al., 2015), demographic classification (Kärkkäinen and Joo, 2021), and measurement of crowd size and violence (Sobolev et al., 2020; Steinert-Threlkeld et al., 2022).

This ground is solid because object recognition tasks are fundamentally about factual coding (e.g., whether a crowd is present in an image), and these tasks tend to produce substantially higher inter-annotator agreement than evaluative ones.⁵ The frontier now lies in evaluative tasks where the question is not *what* the image contains but *what it means*

⁴The argument likely extends to any visual content that engages social or political identity, not only images explicitly labeled as political. An image of a neighborhood, a family, or a workplace can activate group-based evaluative frames just as readily as an image of a protest. What matters is whether the content touches on lines of social division. Images that depict politically inert subject matter (landscapes, nature morte, abstract patterns) are unlikely to produce structured disagreement of this kind.

⁵Even factual image labeling is not free of systematic disagreement. Northcutt et al. (2021) found approximately 6% systematic label errors in the ImageNet validation set, and Beyer et al. (2020) introduced corrected labels after finding that many class boundaries are inherently ambiguous.



Axis	Annotator group 1		Annotator group 2
Party	Democrats ▲	vs.	Republicans
Party × Ethnicity	Hispanic Democrats ▲	vs.	Non-Hisp. Republicans
Party × Age	Young Democrats	vs.	Older Republicans ▲
Within-party (Reps, Ethnicity)	Hispanic Republicans ▲	vs.	Non-Hisp. Republicans
Gender	Women	vs.	Men
Education	≤ B.A.	vs.	> B.A.

▲ = group with higher visual sentiment for this image. Illustrative example. Each row represents one binary comparison between two annotator groups defined along a demographic axis. Some axes produce structured disagreement; others (faded) do not. Whether a given axis yields a meaningful perspective split is itself an empirical question that varies across images.

Figure 1: Illustration of how PVPS classification works. The same image yields structured disagreement across certain demographic axes but not others.

for different people.

Figure 1 illustrates that evaluative disagreement over the same image can emerge along some demographic dimensions but not others. Depending on which identity axis we condition on, a photograph may appear politically divisive, culturally polarized, or largely consensual, meaning that majority-vote labels discard meaningful structure in audience response. Experimental and observational research similarly shows that visual framing can shift political attitudes (Soroka et al., 2016), that media outlets systematically encode events through different visual strategies (Gasparyan and Sirotkina, 2025; Torres, 2021), and that identity-relevant visual cues activate group-specific interpretations (Hiaeshutter-Rice et al., 2023). Modeling these dimensions directly therefore makes it possible to see which lines of disagreement are actually activated by a given image and to measure visual persuasion effects at a more granular level than conventional image-level labels allow.

Gasparyan and Sirotkina (2024) apply this logic to political images directly, training a multi-task model with party-specific classification heads on immigration imagery. This work establishes that perspectivist visual sentiment analysis is feasible and informative. But it, like the cross-domain work reviewed above, fixes a single political dimension in the model architecture.

Webb Williams, Casas, Aslett, et al. (2026) continue this perspectivist logic and show that annotation of political images is sensitive to partisan identity and to demographic characteristics such as gender. Regression results on protest mobilization shift depending on whether labels come from Democrats or Republicans, men or women.

The present work borrows from both of these contributions and develops PVPS classifier that takes the next step:

- The model does not commit to a single social dimension. It computes evaluative divergence along multiple axes simultaneously (partisan, ideological, and demographic) and across their intersections, e.g., young Democrats against old Republi-

cans, high-education Democrats against low-education Democrats, and so on.⁶

- The classifier then learns to predict, from the visual content of the image alone, which side of each divide a given audience segment will fall on.
- The result is a tool that can assess whether an image evokes divergent reactions, along which axes, how confidently the direction of divergence can be predicted from visual content, and whether the fault lines run along partisan, demographic, or intersectional divisions.

Empirical Strategy

PVPS Model Architecture

The most intuitive automated approach today would be to pass each image through a large language model and ask it to simulate audience reactions: “How would a young Democrat feel about this image? How would an old Republican?” But LLMs tend to encode a *default perspective* that reflects the demographic composition of their training data (Santurkar et al., 2023) and embedded stereotypes. When asked to simulate the reactions of specific demographic groups, they can approximate some patterns of opinion variation (Argyle et al., 2023), but the fidelity is uneven, and for visual political content there are few empirical benchmarks tying LLM output to how real people actually responded (Egami et al., 2024).

The classifier developed here learns from what different groups *actually* reported thinking, which is real evaluative divergence measured in survey data and it generalizes that pattern to unseen images. I now describe how this classifier is built.

① **Feature vectors.** Each image is translated into a numerical vector that the classifier

⁶Where the boundary falls on continuous dimensions like age or education is not imposed a priori but searched over empirically, because the location of the fault line is itself part of what needs to be estimated.

can process.⁷ Each image is passed through a set of pretrained models that extract different aspects of its content and encode them as numbers.

I use six extractors because they capture complementary information.⁸ **CLIP** (512 numbers) and **DINOv2** (768 numbers) both produce numerical summaries of what an image looks like, but they learn in different ways. CLIP was trained on hundreds of millions of image–caption pairs, so it encodes visual content together with the symbolic associations carried by language (e.g., a raised fist mapped close to “protest”). DINOv2 was trained on images alone, without any text, so it captures texture, shape, and spatial layout independently of verbal framing.⁹ **Gemini captions** (300 numbers) add an explicit textual layer¹⁰ and these descriptions are converted into numerical vectors via TF-IDF.¹¹ **Semantic features** (50 numbers) are binary indicators of whether specific predictive words appear in the caption, selected per axis and per seed by a chi-squared test on training data.¹² **Concept features** (24 numbers) record the presence or absence of predefined political concepts (protest signs, police, politicians, national symbols, etc.) drawn from the political image literature.¹³ **Political topic features** (12 numbers) indicate which policy domain the image belongs to (immigration, guns, LGBTQ+, climate, etc.), detected from the Gemini description by keyword matching. These six vectors are concatenated into a single 1,666-number fingerprint per image.

⁷For a political-science-oriented introduction to how pretrained models process images, see Torres and Cantú, 2022.

⁸An ablation study (Appendix C) evaluates the contribution of each encoder to classifier performance.

⁹See Appendix F for encoder details.

¹⁰A large language model (Gemini) generates a structured natural-language description of each image (e.g., “a group of people holding signs in front of a government building”). The 300 dimensions correspond to the 300 most informative words in the caption vocabulary.

¹¹TF-IDF (Term Frequency–Inverse Document Frequency) assigns high weight to words that are frequent in a given caption but rare across the corpus. The vocabulary is fitted on the training split only to prevent leakage.

¹²For example, if the word “protest” is strongly associated with one class, the corresponding feature is 1 when that word appears in the caption and 0 otherwise. Unlike TF-IDF, which weights word frequency, these features record presence or absence of specific words selected for their predictive power.

¹³Refined during hyperparameter search to retain only concepts that contributed to classification accuracy. See Appendix G.

- ② **Projection.** These 1,666 numbers contain redundancies and noise. The projection layer compresses them to 256 through a linear transformation followed by layer normalization, forcing the network to retain only the information that matters for predicting group disagreement and discard what does not.
- ③ **Residual Block 1.** The network begins learning which combinations of visual features predict group disagreement. The block transforms the signal through two linear layers with normalization, a nonlinear activation function,¹⁴ and dropout.¹⁵ A skip connection (the dashed line in Figure 2) adds the block’s input directly to its output, so the block only needs to learn a correction to the signal it receives.¹⁶
- ④ **Residual Block 2.** A second block with identical architecture refines the representation further, picking up patterns that the first block missed.¹⁷
- ⑤ **Output head.** The 256-dimensional representation is compressed to 128 through another linear layer with normalization, activation, and dropout, retaining only the features most diagnostic of the final classification.
- ⑥ **Classification.** A final linear layer maps the 128 numbers to class probabilities via softmax. For the standard binary task the output is two probabilities: *consensus* (both groups rate the image similarly) versus *divergence* (one group rates it substantially higher). The image is assigned to whichever class receives the higher probability.¹⁸

¹⁴A function that allows the network to capture relationships that are not simple straight lines. Without it, stacking multiple layers would be equivalent to a single linear transformation.

¹⁵During training, a random fraction of connections is temporarily switched off at each step. This forces the network to spread useful information across many features and prevents it from relying too heavily on any one of them.

¹⁶Skip connections make deeper networks easier to train because adding a block can never make the representation worse. In the worst case, the block learns to output zeros and passes the input through unchanged.

¹⁷Stacking two blocks improved accuracy compared to one; adding a third provided no further gain for data of this size.

¹⁸For multiclass axes (more than two groups), the output layer produces one probability per class and the ensemble averages the full probability distributions across members before assigning the most probable class.

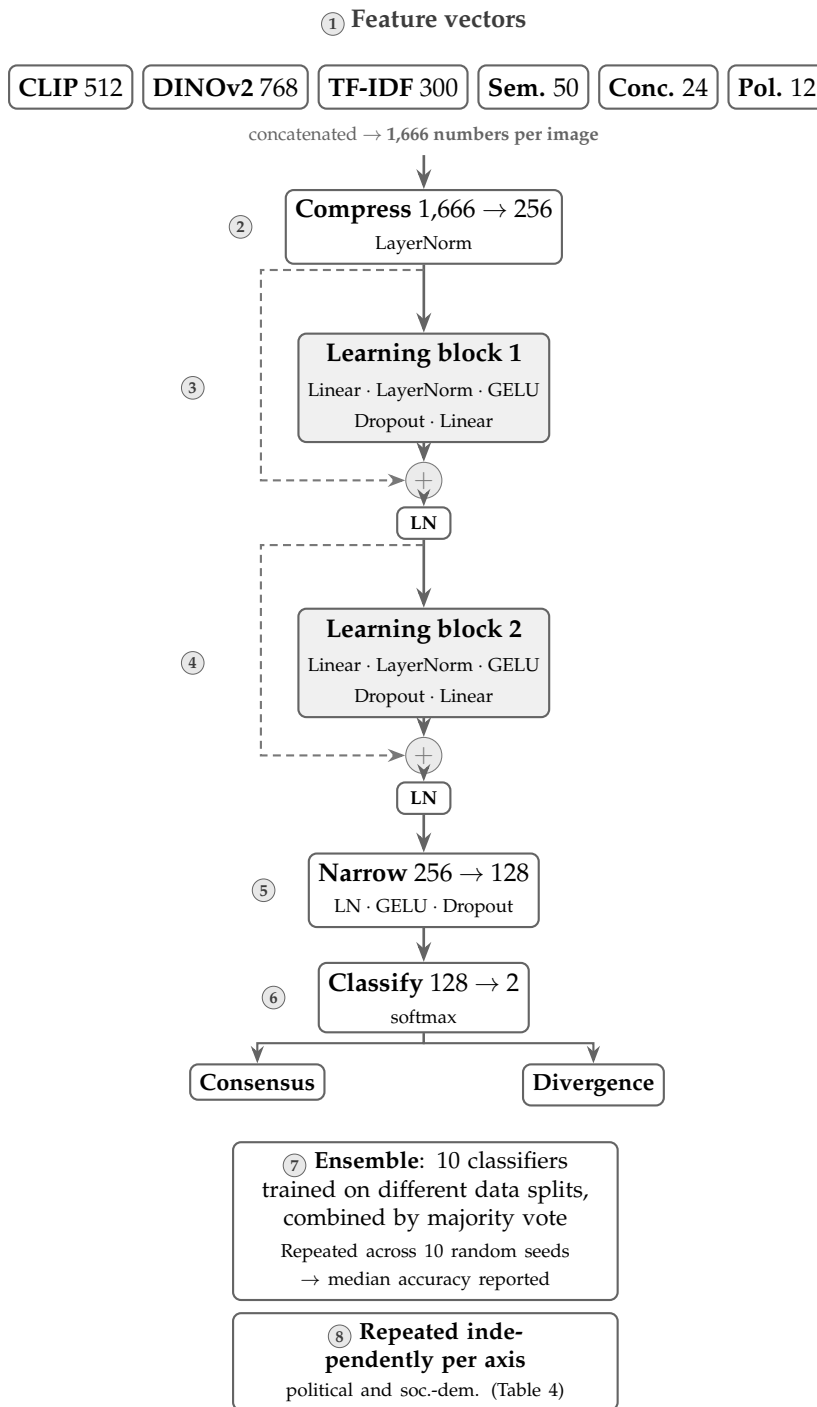
For each axis, the pipeline defines what counts as “divergent” by computing the evaluative gap between groups per image across respondents in the training split and searching over candidate thresholds to find the split that best separates consensual from divisive images.¹⁹

- ⑦ **Ensemble.** No single random split of the data should determine the result. Ten copies of the classifier are trained on different partitions of the data²⁰ and their predictions are combined by majority vote (for binary axes) or by averaging their probability outputs (for multiclass axes). This procedure repeats across ten independent random seeds.²¹ The reported accuracy is the median of the minimum per-class accuracy across seeds, a metric that guards against both lucky splits and classifiers that achieve high overall accuracy by correctly predicting only the more frequent class.
- ⑧ **Repeated independently per axis.** The full pipeline runs separately for each axis and intersection listed in Table 4. Each axis gets its own group boundaries and trained classifier. High accuracy on a given axis means the visual content of the images carries enough information to predict how evaluations will diverge along that social divide. Low accuracy means no such signal is detectable.

¹⁹For continuous variables like age and education, the group boundary itself is part of the search: “young versus old” could mean splitting at 35, 40, or 45, and the pipeline retains whichever definition produces the best class separation on training data. All threshold and boundary decisions are made on the training split only; test images are never used.

²⁰Each partition is stratified, meaning both the training and validation sets preserve the proportion of positive and negative examples found in the full dataset.

²¹A random seed is a number that fixes the sequence of all pseudo-random decisions in the pipeline, such as how data are split and how network weights are initialized. Changing the seed produces a different run of the same experiment. Repeating across multiple seeds tests whether results are stable or depend on a particular sequence of random choices.



What the image looks like (CLIP, DINOv2), what a captioning model says about it (Gemini TF-IDF), which politically diagnostic words appear, which political objects are present, which policy domain

Keep only the information that helps predict who will disagree

Detect which visual patterns predict group divergence. The dashed skip connection preserves the original signal, so the block only needs to learn a correction

Captures subtler patterns the first block missed

Final compression retains only the features most diagnostic for the classification

Does this image divide the two groups, or do they broadly agree? Thresholds for “divisive” are searched on training data only

Ten classifiers vote and the majority decides. The vote is repeated ten times with different random seeds to confirm stability.

Each social divide gets its own classifier. High accuracy = this divide is visually encoded; low accuracy = no detectable signal

Figure 2: Pipeline of PVPS classifier architecture.

Data Sources

The classifier draws on five pools of annotated political images that differ in annotation density, demographic coverage, and the role they play in the pipeline (Table 3).

Table 3: Data sources.

Source	Imgs	Resp.	Annot.	Topics
Wave 1 ^a	356	2,089	16.7K	Immigration
Waves 2+3 ^b	852	4,327	54.9K	Immigration
Wave 4 ^c	412	1,248	27.1K	Immigration, guns, LGBT+, abortion, January 6
Webb Williams et al. (2026) [*]	7,543	~1–3/img	19.8K	Immigration, guns, climate, gender, politics, racial justice, human rights

^aGasparyan and Sirotkina (2025); Lucid, April 2022. A filtered subset of Wave 2 respondents and images, published in *PLOS ONE*.

^bGasparyan and Sirotkina (2024); two Lucid surveys (April 2022 and March 2024).

^cProlific, 2024–2025.

^{*}Webb Williams et al. (2026); Mechanical Turk. Supplementary data, incorporated via semi-supervised self-training (see clarification below).

The primary dataset combines four survey waves (2022–2025, Prolific and Lucid), totaling 1,264 unique images and approximately 82,000 image-by-respondent observations from 5,575 U.S. adults. Waves 1–3 covered immigration (Gasparyan and Sirotkina, 2024; Gasparyan and Sirotkina, 2025); Wave 4 added guns, LGBT+ rights, abortion, and January 6. Each respondent rated images on a 7-point attitude scale and completed a demographic battery (party identification, ideology, feeling thermometers, age, gender, education, income, Hispanic ethnicity). Each image was evaluated by a median of roughly 65 respondents; per-image group comparisons require at least five respondents per group. A supplementary dataset from Webb Williams, Casas, Aslett, et al. (2026) provides 7,543 images rated by MTurk workers on discrete emotions across six policy domains, mapped onto the same 7-point scale via quantile matching ($r=0.917$; partisan-gap sign agreement 92.2%).²² I surveyed several additional datasets, but they lacked the annotator structure

²²Because these data contain only two to three annotators per image, the pipeline incorporates them only through semi-supervised self-training (Lee, 2013; Yarowsky, 1995), pseudo-labeling confident cases (predicted probability ≥ 0.75), with a diagnostic that disables supplementary data if source-classification accuracy exceeds 85%.

necessary for perspectivist classification.²³

Table 4: Classification axes. Each row defines a binary comparison estimated independently by the full pipeline.

Block	Examples
<i>Political</i>	Democrat vs. Republican Liberal vs. Conservative Pro-Democrat vs. Pro-Republican (feeling thermometer)
<i>Demographic</i>	Female vs. Male Hispanic vs. non-Hispanic Young vs. Old; High-ed. vs. Low-ed.; High-inc. vs. Low-inc. ^a
<i>Cross-political</i> × <i>demographic</i>	Young Democrat vs. Old Republican (and reverse) Female Liberal vs. Male Conservative (and reverse) ... both directions for every political–demographic pair ^b
<i>Within-political</i> × <i>demographic</i>	Young Democrat vs. Old Democrat Female Republican vs. Male Republican ... each demographic split within each political group ^c
<i>Same-demographic, cross-political</i>	Young Democrat vs. Young Republican Female Liberal vs. Female Conservative ... same demographic, different political identity ^d

^aFor continuous demographics (age, education, income), the group boundary is searched empirically on training data; the best split (into 2, 3, or 4 groups) is selected automatically.

^bCross-political axes test whether evaluative divergence is detectable when the comparison crosses a political divide and a demographic boundary simultaneously. Both directions are tested, yielding 36 axes across the three political anchors (party, ideology, thermometer).

^cWithin-political axes are diagnostic nulls: if the classifier cannot detect demographic divergence *within* a political group using the same features, the visual signal is political, not demographic. 38 axes total.

^dSame-demographic axes hold the demographic constant and vary only political identity, isolating the partisan component. 30 axes total.

Total: 112 axes.

Table 4 lists the classification axes. The first block captures the partisan divide at varying intensities; the second crosses party with a demographic attribute; the third isolates

²³I surveyed four candidate image datasets that provide individual-level evaluative ratings of political images: Todorov (2017) and Todorov et al. (2005), who collect trait judgments from multiple raters but record no political attributes; Casas and Webb Williams (2019), who collect emotion ratings but with only two to three annotators per image and no demographic battery; and Webb Williams, Casas, and Wilkerson (2020), who record annotator partisanship and gender but again with minimal annotation density per image. Because the perspectivist paradigm (Basile et al., 2021; Cabitza et al., 2023) is not yet standard practice, most political image datasets either aggregate annotations into a single label or discard individual-annotator records entirely, making them unusable for group-conditional training. Only the five sources described above met the pipeline’s requirements, which is individual-level ratings linked to respondent-level political and demographic attributes, with sufficient annotation density per image to estimate group-level evaluative differences.

demographics within each party. This structure reflects stable, overlapping cleavages in American politics, where partisan identity has grown increasingly aligned with ideology and social identity (Boxell et al., 2024; Iyengar, Lelkes, et al., 2019; Mason, 2018), while age, education, gender (Schaffner et al., 2018; Sides et al., 2018), and ethnicity (Hajnal and Lee, 2011; Reny et al., 2019) produce meaningful within-party variation. The within-party axes serve as a diagnostic. If the classifier detects evaluative divergence along a demographic dimension within a party using the same features that work across parties, the signal is at least partly demographic rather than purely partisan.

Results

Overall Classification Performance

Military at Border



LGBTQ+ Rally



January 6



STANDALONE POLITICAL

Party	Dem.	▲ Rep.	▲ Dem.	Rep.	Dem.	▲ Rep.
Ideology	Lib.	▲ Con.	▲ Lib.	Con.	Lib.	▲ Con.
Therm.	Dem-lean.	▲ Rep-lean.	▲ Dem-lean.	Rep-lean.	Dem-lean.	▲ Rep-lean.

SAMESOC-PARTY (same demog., cross-party)

Female×Pty	Fem. Dem.	▲ Fem. Rep.	▲ Fem. Dem.	Fem. Rep.	▲ Fem. Dem.	Fem. Rep.
Old×Pty	Old Dem.	▲ Old Rep.	▲ Old Dem.	Old Rep.	Old Dem.	▲ Old Rep.
HiEd×Pty	HiEd Dem.	▲ HiEd Rep.	▲ HiEd Dem.	HiEd Rep.	HiEd Dem.	▲ HiEd Rep.

TOPIC-SPECIFIC (per-topic sociodem.)

Gender	Female	Male	Female	▲ Male	Female	Male
Hispanic	▲ Hispanic	NonHisp.	▲ Hispanic	NonHisp.	Hispanic	NonHisp.
Age	Young	Old	Young	Old	▲ Young	Old
Education	LowEdu	HighEdu	LowEdu	HighEdu	▲ LowEdu	HighEdu

▲ = group predicted to evaluate this image more positively. Gray = below accuracy threshold.

Figure 3: Evaluative profiles for three held-out images.

Figure 3 displays evaluative profiles for three held-out test images. Full profiles across all 112 axes are reported in Appendix H. On the military-at-border and January 6 images, most political axes align toward Republican, Conservative, and Republican-leaning respondents, while the LGBTQ+ rally reverses this pattern across nearly all political dimensions. Same-sociodemographic cross-party comparisons remain active, showing that partisan disagreement persists even when demographic composition is held constant. In most cases, these cross-party axes follow the broader partisan direction, though January 6 produces some localized reversals, particularly among women.

Political Axes, Demographic Axes, and Their Interaction

Political Axes

The classifier clears the 65% minimum-class accuracy threshold²⁴ on all three primary political axes (see Appendix A.1 for discussion of this threshold). Party identification reaches 68.7% median minimum-class accuracy over ten seeds, ideology reaches 78.9%, and feeling-thermometer difference reaches 78.5%.²⁵

Same-sociodemographic cross-political axes isolate the partisan component by holding demographics constant and varying only political identity. Female Dem. vs. Female Rep. reaches 82.0%, High-education Dem. vs. High-education Rep. 77.2%, Old Liberal vs. Old Conservative 79.7%, and Female Democrat-leaning vs. Female Republican-leaning 77.6%. The partisan signal survives when demographics are equalized.

²⁴A 65% minimum-class accuracy threshold is conservative for a task that predicts subjective evaluative divergence compared to objective image content. Comparable visual political classification tasks achieve 59–72% with far larger datasets and less abstract targets (Kosinski, 2021; Xi et al., 2020), and the threshold here applies to minimum per-class accuracy, which is a stricter criterion than overall accuracy and corresponding to a medium effect size ($d \approx 0.5$) (Yarkoni and Westfall, 2017).

²⁵Throughout the paper, reported accuracy refers to the median over ten independent random seeds of the minimum per-class accuracy on held-out test images. This is the accuracy on whichever class is harder to predict, which guards against classifiers that achieve high overall accuracy by getting only the more common class right. Accuracy on the other class is higher in every case. Full per-class and per-seed results appear in Appendix A. All reported numbers use primary data only. The supplementary dataset was disabled automatically by a pre-training source-prediction diagnostic, since the two image pools are visually distinguishable 97% of the time and a classifier trained on both could learn to separate datasets rather than partisan evaluations (Appendix D).

Sociodemographic Axes

The image-level classifier fails almost uniformly on sociodemographic axes, with median accuracies between 50% and 58% across all thirteen dimensions. That result is substantively plausible given that political images are constructed to communicate political conflict directly, whereas sociodemographic differences are weaker, more conditional, and often entangled with other respondent characteristics.²⁶

To recover this weaker signal, I extend the main PVPS pipeline (Figure 2) with an additional prediction component that conditions on respondent attributes and separates sociodemographic effects from overlapping political structure. Figure 4 illustrates the extended pipeline. Path A is the original image-level classifier and asks whether an image resembles images where one group rated higher than another.²⁷ Path B learns directly from approximately 93,000 individual ratings, modeling how respondent attributes interact with image content while holding other dimensions constant. It estimates whether a given sociodemographic attribute systematically shifts evaluations of particular types of political imagery while avoiding reliance on noisy group-level averages. At test time, the model compares predicted evaluations for two otherwise similar prototypical respondents who differ only on the target dimension, such as age or education.²⁸ A meta-learner combines both paths, learning how much weight to place on the direct visual signal ver-

²⁶If we randomly split the respondents in each group into two halves and compute the gap separately, the two estimates correlate at only $r = 0.20$ for gender and $r = 0.27$ for age, compared to $r = 0.74$ for party. No classifier can predict a target that is 80% noise. Second, the direction of sociodemographic gaps reverses across topics (76% of gun images favoring women, 78% of LGBTQ+ images favoring men), so a pooled classifier encounters contradictory labels for visually similar content.

²⁷On political axes this approach works well because the per-image partisan gap is estimated from roughly thirty Democrats and thirty Republicans and is stable enough to learn from. On the age axis, each group (young vs. old) may contain only seven to ten respondents per image, the resulting gap is 80% sampling noise, and Path A has little to learn. The set of visual encoders fed into Path A is tailored per axis in a prior ablation study (Appendix C), because including all six feature sources at once introduces noise that drowns out the weaker sociodemographic signal. For example, the age axis uses SigLIP with DINOv2 and caption features; the education axis uses concept indicators with handcrafted political features. These combinations were fixed before the main evaluation.

²⁸This is analogous to a regression with interaction terms ($\text{rating} \sim \text{image features} \times \text{respondent age}$), estimated on 93,000 observations rather than on 1,264 noisy per-image means of seven respondents each.

sus the respondent-conditioned signal for each axis.²⁹

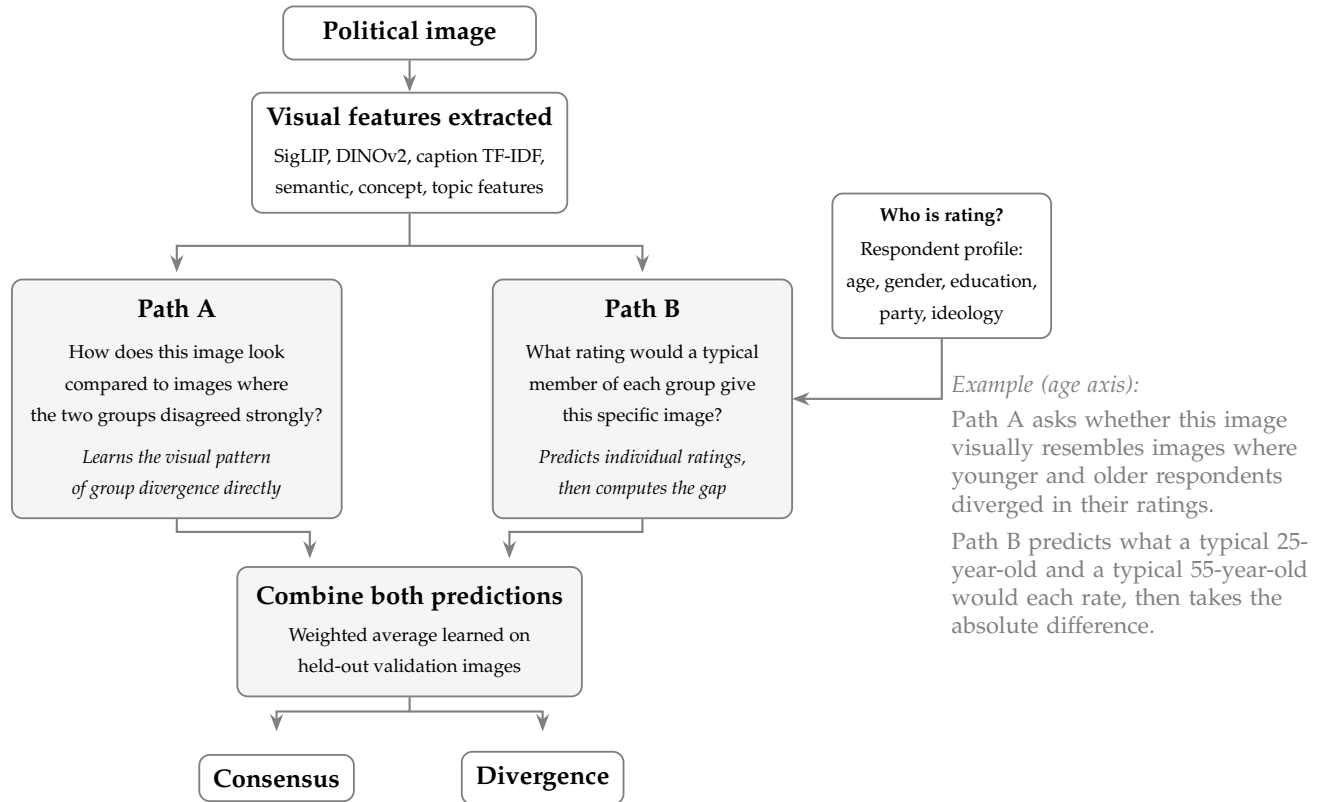


Figure 4: Extended pipeline for sociodemographic axes. The main PVPS classifier (Figure 2) fails on sociodemographic dimensions because the per-image evaluative gaps are too noisy. This extension combines two complementary prediction strategies per axis. Path A predicts the evaluative gap from visual content alone. Path B predicts individual ratings from image features and respondent attributes, then derives the gap. A weighted combination learned on validation data produces the final classification.

Under this extended pipeline, eight sociodemographic axes exceed 60% median minimum-class accuracy. Age reaches 68.9% ($r = 0.619$), gender 62.0% ($r = 0.489$), and education 61.0% ($r = 0.419$), with several within-party and within-ideology age comparisons also producing stable signal.³⁰ These results suggest that social identity does shape evalua-

²⁹Ridge regression fitted on held-out validation images. On political axes Path A dominates because the per-image gap is reliable; on sociodemographic axes Path B contributes more because it extracts signal from individual ratings that the per-image gap is too noisy to preserve. Decision thresholds are calibrated on validation data only, and ten independent random seeds assess stability.

³⁰The remaining sociodemographic axes fall between 42% and 59%. Income produces no signal on any formulation. Hispanic ethnicity axes do not reach meaningful accuracy, consistent with their low split-half reliability ($r = 0.11$). Within-party, within-ideology, and within-thermometer gender and education axes

tions of political imagery, but the visual signal is substantially weaker and more conditional than the partisan signal. Recovering it requires conditioning on overlapping respondent characteristics rather than relying on image-level disagreement alone.

Model Application

The classifier was trained and evaluated on survey data mainly collected more or less for this study. To test whether it produces meaningful predictions on images it has never seen, I apply it to two published datasets and ask whether the PVPS evaluative profiles change the substantive conclusions those studies report.

Casas and Webb Williams (2019)

Casas and Webb Williams (2019) collect 150,000 BLM tweets (9,500 images, ShutdownA14, April 2015) and have 1,259 MTurk workers rate each image on five emotions (0–10).³¹ Negative binomial regressions predicting retweet count show that enthusiasm and fear increase engagement while sadness decreases it (Figure 5, top row, replicated from their data). The emotion scores are averaged across annotators and treated as fixed properties of each image.

I run the same 8,013 images through the PVPS classifier, producing predicted probabilities for each passing axis. I then interact each emotion score with the PVPS probability to test whether the mobilizing effect of a given emotion depends on which group the image favors. The interaction model takes the form

$$\text{retweets} \sim \text{emotion}_j + \text{PVPS}_k + \text{emotion}_j \times \text{PVPS}_k + \text{controls} \quad (1)$$

also remain near chance.

³¹The top ~950 most-retweeted images were each labeled by five annotators (two undergraduate research assistants and three MTurk workers), with the emotion score averaged across the five. The remaining 8,509 images were labeled by a single annotator drawn from a pool of 1,259 MTurk workers, each of whom could label at most 100 images (Casas and Webb Williams, 2019, pp. 367–68).

estimated separately for each emotion j and PVPS axis k , with the same controls as the original specification (log followers, log friends, log previous tweets, time fixed effects).

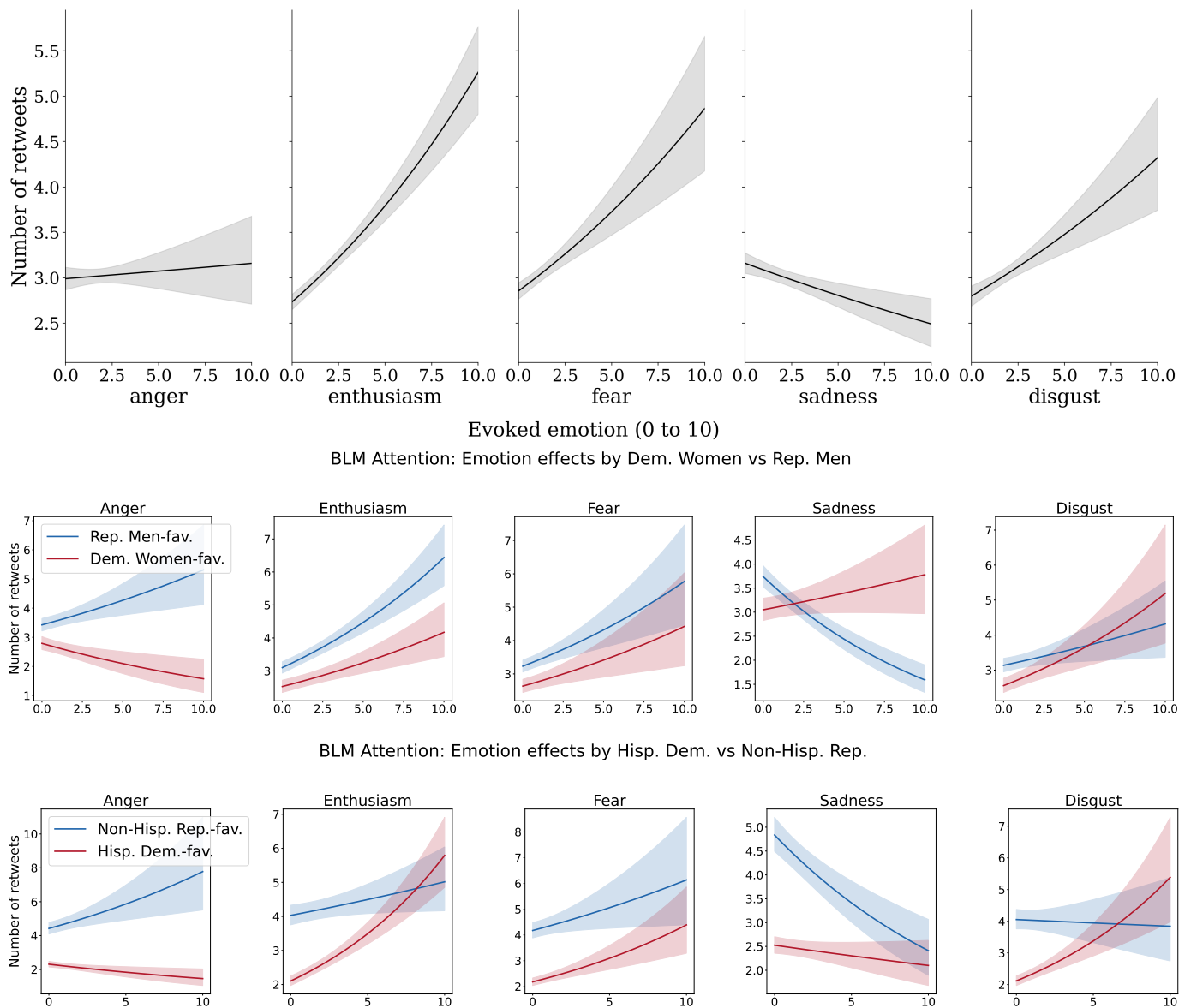


Figure 5: Predicting attention to BLM images over the range of evoked emotions. Top row replicates Casas and Webb Williams (2019, Figure 6), showing predicted retweet counts as a function of emotion intensity (0–10) with 95% confidence bands. Middle row splits predicted retweets by PVPS score on the Democratic Women vs. Republican Men axis (blue = Republican-men-favorable images, red = Democratic-women-favorable). Bottom row splits by the Hispanic Democrat vs. Non-Hispanic Republican axis. Diverging lines indicate that the mobilizing effect of a given emotion depends on the partisan-demographic perspective the image conveys. All models are negative binomial with the same controls as the original specification. Confidence bands are computed via the delta method.

The middle and bottom rows of Figure 5 show predicted retweet counts as emotions vary from 0 to 10, separately for images classified as favorable to one group or the other. On the Democratic Women vs. Republican Men axis, enthusiasm produces a steeper positive slope for Democrat-women-favorable images, while fear and disgust generate stronger engagement for Republican-men-favorable images. Sadness depresses engagement asymmetrically, mainly for Republican-men-favorable content.

The Hispanic Democrat vs. Non-Hispanic Republican axis shows the same qualitative structure, though with wider confidence intervals due to the smaller effective sample size. Across additional intersectional axes (Appendix H), emotional effects consistently depend on which group the image is perceived to favor. Enthusiasm mobilizes aligned audiences, while fear and disgust amplify engagement with threatening outgroup content, patterns obscured by averaged emotion scores alone.

Won, Steinert-Threlkeld, and Joo (2017)

Won, Steinert-Threlkeld, and Joo (2017) release the UCLA Protest Image Dataset (40,764 images, 11,659 protest) annotated for binary protest presence, ten visual attributes, and continuous perceived violence via Bradley-Terry pairwise comparisons. Their Table 4 (of the original article) reports that fire ($r = +.59$) and law enforcement ($r = +.37$) predict higher perceived violence, while signs ($r = -.49$) predict lower violence. These correlations are treated as properties of the images themselves. The annotators' demographics are not recorded.

I run 2,343 held-out protest test images (none in the PVPS training data) through the PVPS classifier and correlate each axis probability with perceived violence. Figure 6 shows the results side by side. The left panel replicates Won et al.'s findings on the test set. The right panel shows that every PVPS axis correlates positively with violence, with the strongest effects on cross-party axes (Low-income Dem. vs. High-income Rep. $r = +.588$, Non-Hispanic Dem. vs. Non-Hispanic Rep. $r = +.518$, Dem.-leaning Con.

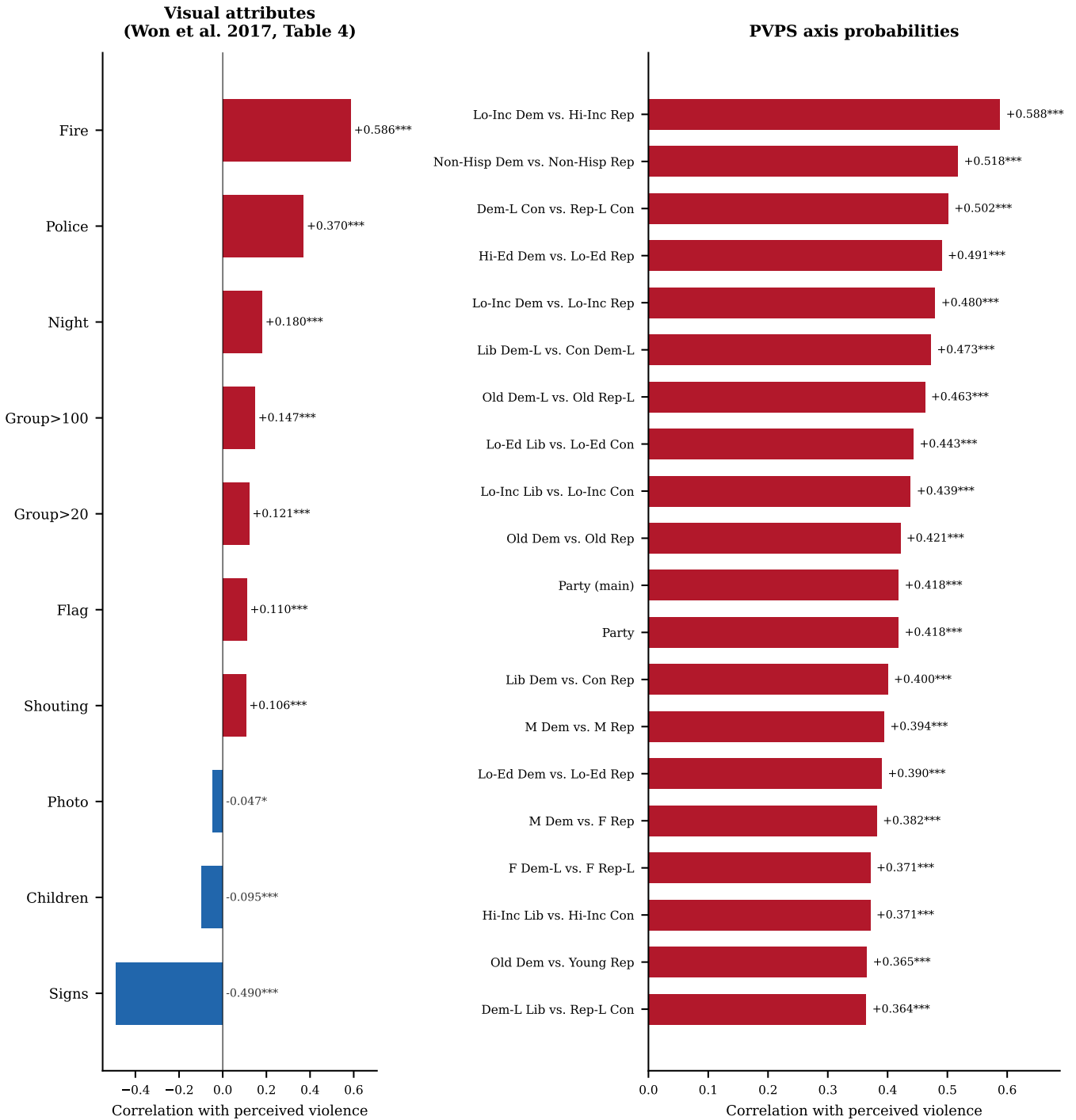


Figure 6: Correlates of perceived violence in protest images ($n = 2,343$, UCLA Protest Image Dataset test set). Left panel replicates Won et al. (2017) Table 4 showing correlations between visual attributes and perceived violence. Right panel shows correlations between PVPS axis probabilities and the same violence scores. All PVPS axes correlate positively with violence, meaning images perceived as more violent are the same images the PVPS classifier predicts as more favorably evaluated by Republican, conservative, and Republican-leaning respondents. *** $p < .001$, ** $p < .01$, * $p < .05$.

vs. Rep.-leaning Con. $r = +.502$, all $p < .001$). The primary party axis reaches $r = +.418$. The weakest effect appears on the Dem.-leaning Lib. vs. Rep.-leaning Con. axis ($r = +.364$), but all axes are significant at $p < .001$. Images that the PVPS classifier predicts as more favorably evaluated by Republicans, conservatives, and Republican-leaning respondents are also the images that Won et al.'s annotators rate as more violent, while images with protest signs and peaceful marches are predicted as more favorably evaluated by Democrats and liberals.

This suggests that perceived violence in protest imagery is not politically neutral but follows the same partisan fault lines that structure political evaluation. Features such as fire and police presence characterize images aligned with conservative audiences, whereas protest signs characterize images aligned with liberal audiences. Because the MTurk annotator pool used by Won et al. did not record political demographics, the dataset cannot test whether Democrats and Republicans assign different violence ratings to the same images, a question that a perspectivist annotation design could directly address. Importantly, these results do not invalidate their findings but add an additional layer of structure by showing that visual attributes, audience identity, and evaluative outcomes jointly shape perceived violence.

Discussion and Limitations

Political science has long argued that evaluative disagreement is structured by identity and social location (Campbell et al., 1960; Kinder and Kam, 2009; Mason, 2018). Computational social science has extended this tradition by applying computer vision and NLP tools to classify political content at scale (Grimmer, Roberts, et al., 2022; Joo and Steinert-Threlkeld, 2022; Won et al., 2017), but these methods were primarily designed for tasks with a single correct label and therefore collapse annotator disagreement by construction (Cabitz et al., 2023; Uma et al., 2021). As a result, they are well suited for prediction tasks

but less suited for studying the structure of disagreement itself.

PVPS addresses this gap by turning evaluative disagreement into the object of prediction. It embeds perspectivist assumptions from political science directly into a computational model, which makes structured disagreement both observable and predictable from image content. However, several design choices constrain what this approach can recover, and these constraints point to clear directions for future work:

Soft labels as an alternative architecture: The PVPS classifier trains a separate binary model for each social axis. An alternative would be to train a single model on the full distribution of annotator responses, known as soft-label training, where the model receives the proportion of annotators who chose each option rather than a single collapsed answer. Soft-label approaches have shown advantages in subjective NLP tasks (Fornaciari et al., 2021; Peterson et al., 2019; Rodrigues and Pereira, 2018; Uma et al., 2021). I chose per-group classifiers because a soft-label distribution captures *that* annotators disagree but not *who* disagrees with whom. This means that an image where Democrats and Republicans split 60/40 in opposite directions produces the same bimodal shape as one where young and old split identically. Per-group classifiers keep the social identity of the disagreement visible (Mostafazadeh Davani et al., 2022). A hybrid architecture combining distributional training with group-specific heads is a natural next step.

Dataset scale: The primary dataset contains 1,264 images and 82,000 observations. The classifier operates on frozen CLIP and DINOv2 representations pretrained on hundreds of millions of images, so the classification head only learns which feature combinations predict group disagreement. Transfer learning at this scale has proven effective in political science (Joo and Steinert-Threlkeld, 2022; Kornblith et al., 2019; Radford et al., 2021; Xi et al., 2020), and U.S. partisan effect sizes are large ($d \approx 1.0$ – 1.7 ; Iyengar and Westwood, 2015), meaning the groups are far apart to begin with. The uniform within-party null results confirm the classifier is not picking up noise. More images would sharpen the analysis, but the core partisan signal is strong enough at this scale.

Other possible social axes: Religion (Layman and Carmines, 1997), geography (Rodden, 2019), media consumption (Prior, 2007), and moral foundations (Graham et al., 2009) all structure political attitudes in ways that should matter for image evaluation. Some are partially absorbed by included axes (religiosity correlates with partisanship; geography with education and income). The selection I made follows theory-driven variable choice, but the framework is modular. So any axis can be added given annotator-level data, and whether it matters empirically is itself a finding the classifier produces.

Higher-order intersections: The classifier models pairwise intersections but not three-way (or x-way) combinations. Intersectionality theory motivates attention to joint identity categories (Crenshaw, 1991; McCall, 2005), but detecting a two-way interaction already requires roughly sixteen times the sample size of a main effect (Gelman, 2018; McClelland and Judd, 1993). In practice, two-way intersections capture the most consequential disparities (Buolamwini and Gebru, 2018; Kearns et al., 2018). Larger datasets would make selected three-way intersections feasible, and the pipeline accommodates them without architectural changes.

Generalizability: The U.S. is an affective-polarization outlier among OECD democracies (Boxell et al., 2024), its two-party system and media environment operate under dynamics that do not transfer straightforwardly to multiparty settings (Dalton, 2008; Hallin and Mancini, 2004), and cross-cultural research in cognitive psychology suggests that even basic visual perception is shaped by cultural context (Henrich et al., 2010; Nisbett and Miyamoto, 2005). The principle that stable social cleavages produce structured disagreement should hold across contexts (Kriesi et al., 2008; Lipset and Rokkan, 1967), but the images that activate them will differ, since topics like Black Lives Matter are specifically American.

Who will use PVPS? Across social media research (Barberá, 2015; Brady et al., 2017; Guess et al., 2023; Jia et al., 2025), PVPS turns image flows into group-conditioned evaluative profiles, making it possible to test whether amplification favors content that increases

consensus within groups or divergence across them. In studies of visual framing by news outlets (Gasparyan and Sirotkina, 2025; Geise and Xu, 2025; Peng, 2018), the unit of analysis shifts from what is shown to how different audience segments respond. This allows outlet strategies to be evaluated in terms of anticipated audience polarization. Work on visual misinformation (Hameleers et al., 2024; Yang et al., 2023) can rank images by expected disagreement across groups and identify those most likely to generate partisan split rather than generic false belief. In experimental research (Hiaeshutter-Rice et al., 2023), the same mechanism removes the need for iterative pretesting by scoring candidate stimuli directly in terms of expected audience structure.

More generally, PVPS replaces post hoc stimulus selection with a pre-measured mapping of expected evaluative disagreement across social groups. This makes it possible to design visual experiments from the structure of audience disagreement itself.

References

- Achen, Christopher H. and Larry M. Bartels (2016). *Democracy for Realists: Why Elections Do Not Produce Responsive Government*. Princeton, NJ: Princeton University Press.
- Argyle, Lisa P. et al. (2023). “Out of One, Many: Using Language Models to Simulate Human Samples”. In: *Political Analysis* 31.3.
- Aroyo, Lora and Chris Welty (2015). “Truth Is a Lie: Crowd Truth and the Seven Myths of Human Annotation”. In: *AI Magazine* 36.1, pp. 15–24. DOI: [10.1609/aimag.v36i1.2564](https://doi.org/10.1609/aimag.v36i1.2564).
- Barberá, Pablo (2015). “Birds of the Same Feather Tweet Together: Bayesian Ideal Point Estimation Using Twitter Data”. In: *Political Analysis* 23.1, pp. 76–91. DOI: [10.1093/pan/mpu011](https://doi.org/10.1093/pan/mpu011).
- Barberá, Pablo et al. (2015). “Tweeting From Left to Right: Is Online Political Communication More Than an Echo Chamber?” In: *Psychological Science* 26.10, pp. 1531–1542. DOI: [10.1177/0956797615594620](https://doi.org/10.1177/0956797615594620).
- Barocas, Solon and Andrew D. Selbst (2016). “Big Data’s Disparate Impact”. In: *California Law Review* 104.3, pp. 671–732.
- Bartolini, Stefano and Peter Mair (1990). *Identity, Competition, and Electoral Availability: The Stabilisation of European Electorates, 1885–1985*. Cambridge: Cambridge University Press.
- Basile, Valerio et al. (2021). “We Need to Consider Disagreement in Evaluation”. In: *Proceedings of the 1st Workshop on Benchmarking: Past, Present and Future*, pp. 15–21.
- Benoit, Kenneth et al. (2016). “Crowd-sourced Text Analysis: Reproducible and Agile Production of Political Data”. In: *American Political Science Review* 110.2, pp. 278–295.
- Berger, Peter L. and Thomas Luckmann (1966). *The Social Construction of Reality: A Treatise in the Sociology of Knowledge*. Garden City, NY: Doubleday.

- Bestvater, Samuel and Brendan Monroe (2023). "Sentiment is Not Stance: Target-Aware Opinion Classification for Political Text Analysis". In: *Political Analysis* 31.2, pp. 235–256. DOI: [10.1017/pan.2022.10](https://doi.org/10.1017/pan.2022.10).
- Beyer, Lucas et al. (2020). *Are We Done with ImageNet?* arXiv: [2006.07159](https://arxiv.org/abs/2006.07159).
- Boxell, Levi, Matthew Gentzkow, and Jesse M. Shapiro (2024). "Cross-Country Trends in Affective Polarization". In: *Review of Economics and Statistics* 106.2, pp. 557–565.
- Brady, William J. et al. (2017). "Emotion Shapes the Diffusion of Moralized Content in Social Networks". In: *Proceedings of the National Academy of Sciences* 114.28, pp. 7313–7318.
- Buolamwini, Joy and Timnit Gebru (2018). "Gender Shades: Intersectional Accuracy Disparities in Commercial Gender Classification". In: *Proceedings of the 1st Conference on Fairness, Accountability and Transparency (EAT*)*. PMLR 81, pp. 77–91.
- Cabitza, Federico, Andrea Campagner, and Valerio Basile (2023). "Toward a Perspectivist Turn in Ground Truthing for Predictive Computing". In: *Proceedings of the AAAI Conference on Artificial Intelligence*. Vol. 37. 6, pp. 6860–6868. DOI: [10.1609/aaai.v37i6.25840](https://doi.org/10.1609/aaai.v37i6.25840).
- Campbell, Angus et al. (1960). *The American Voter*. New York: John Wiley & Sons.
- Casas, Andreu and Nora Webb Williams (2019). "Images that Matter: Online Protests and the Mobilizing Role of Pictures". In: *Political Research Quarterly* 72.2, pp. 360–375. DOI: [10.1177/1065912918786805](https://doi.org/10.1177/1065912918786805).
- Converse, Philip E. (1964). "The Nature of Belief Systems in Mass Publics". In: *Ideology and Discontent*. Ed. by David E. Apter. New York: The Free Press, pp. 206–261.
- Crenshaw, Kimberlé (1991). "Mapping the Margins: Intersectionality, Identity Politics, and Violence Against Women of Color". In: *Stanford Law Review* 43.6, pp. 1241–1299.
- Dalton, Russell J. (2008). "The Quantity and the Quality of Party Systems: Party System Polarization, Its Measurement, and Its Consequences". In: *Comparative Political Studies* 41.7, pp. 899–920. DOI: [10.1177/0010414008315860](https://doi.org/10.1177/0010414008315860).

- Dugger, Karen (1988). “Social Location and Gender-Role Attitudes: A Comparison of Black and White Women”. In: *Gender and Society* 2.4, pp. 425–448.
- Dumitrache, Anca, Lora Aroyo, and Chris Welty (2018). “Crowdsourcing Ground Truth for Medical Relation Extraction”. In: *ACM Transactions on Interactive Intelligent Systems* 8.2, Article 11, 1–20. DOI: [10.1145/3152889](https://doi.org/10.1145/3152889).
- Egami, Naoki et al. (2024). “Using Imperfect Surrogates for Downstream Inference: Design-based Supervised Learning for Social Science Applications of Large Language Models”. In: *Advances in Neural Information Processing Systems (NeurIPS)*. Vol. 36, pp. 68589–68601.
- Fleisig, Eve, Rediet Abebe, and Dan Klein (2023). “When the Majority is Wrong: Modeling Annotator Disagreement for Subjective Tasks”. In: *Proceedings of EMNLP 2023*. Singapore: ACL, pp. 6715–6726. DOI: [10.18653/v1/2023.emnlp-main.415](https://doi.org/10.18653/v1/2023.emnlp-main.415).
- Flora, Peter, Stein Kuhnle, and Derek Urwin (1999). *State Formation, Nation-Building, and Mass Politics in Europe: The Theory of Stein Rokkan*. Oxford: Oxford University Press.
- Fornaciari, Tommaso et al. (2021). “Beyond Black & White: Leveraging Annotator Disagreement via Soft-Label Multi-Task Learning”. In: *Proceedings of the 2021 Conference of the North American Chapter of the Association for Computational Linguistics: Human Language Technologies*. ACL, pp. 2591–2597.
- Frenda, Simona et al. (2025). “Perspectivist Approaches to Natural Language Processing: A Survey”. In: *Language Resources and Evaluation* 59, pp. 1719–1746. DOI: [10.1007/s10579-024-09766-4](https://doi.org/10.1007/s10579-024-09766-4).
- Gasparyan, Olga and Elena Sirotkina (2024). *Decoding Visual Sentiment of Political Imagery*. arXiv: [2408.04103](https://arxiv.org/abs/2408.04103).
- (2025). “Media Choice and Audience Perceptions: Evidence from Visual Framing of Immigration in News Stories”. In: *PLOS ONE* 20.9, e0331219. DOI: [10.1371/journal.pone.0331219](https://doi.org/10.1371/journal.pone.0331219).

- Geise, Stephanie and Yi Xu (2025). “Effects of Visual Framing in Multimodal Media Environments: A Systematic Review of Studies Between 1979 and 2023”. In: *Journalism & Mass Communication Quarterly* 102.3, pp. 796–823. DOI: [10.1177/10776990241257586](https://doi.org/10.1177/10776990241257586).
- Gelman, Andrew (2018). *You Need 16 Times the Sample Size to Estimate an Interaction Than to Estimate a Main Effect*. Statistical Modeling, Causal Inference, and Social Science (blog), March 15. See also Gelman, Hill, and Vehtari (2020), *Regression and Other Stories*, Section 16.4.
- Goyal, Nitesh et al. (2022). “Is Your Toxicity My Toxicity? Exploring the Impact of Rater Identity on Toxicity Annotation”. In: *Proceedings of the ACM on Human-Computer Interaction* 6.CSCW2, Article 406, 1–28. DOI: [10.1145/3555088](https://doi.org/10.1145/3555088).
- Graham, Jesse, Jonathan Haidt, and Brian A. Nosek (2009). “Liberals and Conservatives Rely on Different Sets of Moral Foundations”. In: *Journal of Personality and Social Psychology* 96.5, pp. 1029–1046. DOI: [10.1037/a0015141](https://doi.org/10.1037/a0015141).
- Grimmer, Justin, Margaret E. Roberts, and Brandon M. Stewart (2022). *Text as Data: A New Framework for Machine Learning and the Social Sciences*. Princeton University Press.
- Grimmer, Justin and Brandon M. Stewart (2013). “Text as Data: The Promise and Pitfalls of Automatic Content Analysis Methods for Political Texts”. In: *Political Analysis* 21.3, pp. 267–297. DOI: [10.1093/pan/mps028](https://doi.org/10.1093/pan/mps028).
- Guess, Andrew M. et al. (2023). “How Do Social Media Feed Algorithms Affect Attitudes and Behavior in an Election Campaign?” In: *Science* 381.6656, pp. 398–404.
- Haidt, Jonathan (2012). *The Righteous Mind: Why Good People Are Divided by Politics and Religion*. New York: Pantheon Books.
- Hajnal, Zoltan L. and Taeku Lee (2011). *Why Americans Don’t Join the Party: Race, Immigration, and the Failure (of Political Parties) to Engage the Electorate*. Princeton University Press.
- Hallin, Daniel C. and Paolo Mancini (2004). *Comparing Media Systems: Three Models of Media and Politics*. Cambridge University Press. DOI: [10.1017/CBO9780511790867](https://doi.org/10.1017/CBO9780511790867).

- Hameleers, Michael, Toni G. L. A. van der Meer, and André Krouwel (2024). "The Nature of Visual Disinformation Online: A Qualitative Content Analysis of Alternative and Social Media in the Netherlands". In: *Political Communication* 42.1, pp. 1–22.
- Hancock, Ange-Marie (2007). "When Multiplication Doesn't Equal Quick Addition: Examining Intersectionality as a Research Paradigm". In: *Perspectives on Politics* 5.1, pp. 63–79. DOI: [10.1017/S1537592707070065](https://doi.org/10.1017/S1537592707070065).
- Henrich, Joseph, Steven J. Heine, and Ara Norenzayan (2010). "The Weirdest People in the World?" In: *Behavioral and Brain Sciences* 33.2–3, pp. 61–83. DOI: [10.1017/S0140525X0999152X](https://doi.org/10.1017/S0140525X0999152X).
- Hiaeshutter-Rice, Dan, Fabian G. Neuner, and Stuart Soroka (2023). "Cued by Culture: Political Imagery and Partisan Evaluations". In: *Political Behavior* 45.2, pp. 741–759. DOI: [10.1007/s11109-021-09726-6](https://doi.org/10.1007/s11109-021-09726-6).
- Hooghe, Liesbet, Gary Marks, and Carole J. Wilson (2002). "Does Left/Right Structure Party Positions on European Integration?" In: *Comparative Political Studies* 35.8, pp. 965–989. DOI: [10.1177/001041402236310](https://doi.org/10.1177/001041402236310).
- Huckfeldt, Robert and John Sprague (1995). *Citizens, Politics, and Social Communication: Information and Influence in an Election Campaign*. Cambridge University Press. DOI: [10.1017/CBO9780511664113](https://doi.org/10.1017/CBO9780511664113).
- Iyengar, Shanto, Yphtach Lelkes, et al. (2019). "The Origins and Consequences of Affective Polarization in the United States". In: *Annual Review of Political Science* 22, pp. 129–146.
- Iyengar, Shanto and Sean J. Westwood (2015). "Fear and Loathing across Party Lines: New Evidence on Group Polarization". In: *American Journal of Political Science* 59.3, pp. 690–707. DOI: [10.1111/ajps.12152](https://doi.org/10.1111/ajps.12152).
- Jardina, Ashley (2019). *White Identity Politics*. Cambridge University Press.
- Jennings, M. Kent and Richard G. Niemi (1981). *Generations and Politics: A Panel Study of Young Adults and Their Parents*. Princeton, NJ: Princeton University Press. DOI: [10.1515/9781400854264](https://doi.org/10.1515/9781400854264).

- Jia, Tiziano et al. (2025). “Reranking Partisan Animosity in Algorithmic Social Media Feeds Alters Affective Polarization”. In: *Science*.
- Joo, Jungseock, Francis F. Steen, and Song-Chun Zhu (2015). “Automated Facial Trait Judgment and Election Outcome Prediction: Social Dimensions of Face”. In: *Social Science Computer Review* 33.6, pp. 712–727.
- Joo, Jungseock and Zachary C. Steinert-Threlkeld (2022). “Image as Data: Automated Visual Content Analysis for Political Science”. In: *Computational Communication Research* 4.1. arXiv preprint 1810.01544, 2018.
- Kahan, Dan M. (2013). “Ideology, Motivated Reasoning, and Cognitive Reflection”. In: *Judgment and Decision Making* 8.4, pp. 407–424.
- Kärkkäinen, Kimmo and Jungseock Joo (2021). “FairFace: Face Attribute Dataset for Balanced Race, Gender, and Age for Bias Measurement and Mitigation”. In: *Proceedings of the IEEE/CVF Winter Conference on Applications of Computer Vision (WACV)*, pp. 1548–1558.
- Kearns, Michael et al. (2018). “Preventing Fairness Gerrymandering: Auditing and Learning for Subgroup Fairness”. In: *Proceedings of the 35th International Conference on Machine Learning (ICML)*. PMLR 80, pp. 2564–2572.
- Kinder, Donald R. and Cindy D. Kam (2009). *Us Against Them: Ethnocentric Foundations of American Opinion*. Chicago: University of Chicago Press.
- Kornblith, Simon, Jonathon Shlens, and Quoc V. Le (2019). “Do Better ImageNet Models Transfer Better?” In: *Proceedings of the IEEE/CVF Conference on Computer Vision and Pattern Recognition (CVPR)*, pp. 2661–2671. DOI: [10.1109/CVPR.2019.00277](https://doi.org/10.1109/CVPR.2019.00277).
- Kosinski, Michal (2021). “Facial recognition technology can expose political orientation from naturalistic facial images”. In: *Scientific Reports* 11.1, p. 100. DOI: [10.1038/s41598-020-79310-1](https://doi.org/10.1038/s41598-020-79310-1).
- Kriesi, Hanspeter et al. (2008). *West European Politics in the Age of Globalization*. Cambridge University Press. DOI: [10.1017/CBO9780511790720](https://doi.org/10.1017/CBO9780511790720).

- Layman, Geoffrey C. and Edward G. Carmines (1997). "Cultural Conflict in American Politics: Religious Traditionalism, Postmaterialism, and U.S. Political Behavior". In: *The Journal of Politics* 59.3, pp. 751–777. DOI: [10.2307/2998636](https://doi.org/10.2307/2998636).
- Lee, Dong-Hyun (2013). "Pseudo-Label: The Simple and Efficient Semi-Supervised Learning Method for Deep Neural Networks". In: *ICML 2013 Workshop: Challenges in Representation Learning*. Atlanta.
- Lipset, Seymour Martin and Stein Rokkan (1967). "Cleavage Structures, Party Systems, and Voter Alignments: An Introduction". In: *Party Systems and Voter Alignments: Cross-National Perspectives*. Ed. by Seymour Martin Lipset and Stein Rokkan. New York: The Free Press, pp. 1–64.
- Lucas, Christopher et al. (2015). "Computer-assisted text analysis for comparative politics". In: *Political Analysis* 23.2, pp. 254–277.
- Mannheim, Karl (1936). *Ideology and Utopia: An Introduction to the Sociology of Knowledge*. Trans. by Louis Wirth and Edward Shils. New York: Harcourt, Brace & Co.
- Mason, Lilliana (2018). *Uncivil Agreement: How Politics Became Our Identity*. Chicago: University of Chicago Press.
- McCall, Leslie (2005). "The Complexity of Intersectionality". In: *Signs: Journal of Women in Culture and Society* 30.3, pp. 1771–1800. DOI: [10.1086/426800](https://doi.org/10.1086/426800).
- McClelland, Gary H. and Charles M. Judd (1993). "Statistical Difficulties of Detecting Interactions and Moderator Effects". In: *Psychological Bulletin* 114.2, pp. 376–390. DOI: [10.1037/0033-2909.114.2.376](https://doi.org/10.1037/0033-2909.114.2.376).
- Mehrabi, Ninareh et al. (2021). "A Survey on Bias and Fairness in Machine Learning". In: *ACM Computing Surveys* 54.6, Article 115, 1–35. DOI: [10.1145/3457607](https://doi.org/10.1145/3457607).
- Mikhaylov, Slava, Michael Laver, and Kenneth R. Benoit (2012). "Coder Reliability and Misclassification in the Human Coding of Party Manifestos". In: *Political Analysis* 20.1, pp. 78–91.

- Mostafazadeh Davani, Aida, Mark Díaz, and Vinodkumar Prabhakaran (2022). “Dealing with Disagreements: Looking Beyond the Majority Vote in Subjective Annotations”. In: *Transactions of the Association for Computational Linguistics* 10, pp. 92–110. DOI: [10.1162/tacl_a_00449](https://doi.org/10.1162/tacl_a_00449).
- Mouffe, Chantal (2005). *On the Political*. London: Routledge. DOI: [10.4324/9780203870112](https://doi.org/10.4324/9780203870112).
- Nisbett, Richard E. and Yuri Miyamoto (2005). “The Influence of Culture: Holistic versus Analytic Perception”. In: *Trends in Cognitive Sciences* 9.10, pp. 467–473. DOI: [10.1016/j.tics.2005.08.004](https://doi.org/10.1016/j.tics.2005.08.004).
- Northcutt, Curtis G., Anish Athalye, and Jonas Mueller (2021). “Pervasive Label Errors in Test Sets Destabilize Machine Learning Benchmarks”. In: *Proceedings of the 35th Conference on Neural Information Processing Systems (NeurIPS), Datasets and Benchmarks Track*.
- Orlikowski, Matthias et al. (2023). “The Ecological Fallacy in Annotation: Modeling Human Label Variation Goes beyond Sociodemographics”. In: *Proceedings of the 61st ACL (Volume 2: Short Papers)*. Toronto: ACL, pp. 1017–1029. DOI: [10.18653/v1/2023.acl-short.88](https://doi.org/10.18653/v1/2023.acl-short.88).
- Pavlick, Ellie and Tom Kwiatkowski (2019). “Inherent Disagreements in Human Textual Inferences”. In: *Transactions of the Association for Computational Linguistics* 7, pp. 677–694. DOI: [10.1162/tacl_a_00293](https://doi.org/10.1162/tacl_a_00293).
- Peng, Yilang (2018). “Same Candidates, Different Faces: Uncovering Media Bias in Visual Portrayals of Presidential Candidates with Computer Vision”. In: *Journal of Communication* 68.5, pp. 920–941. DOI: [10.1093/joc/jqy041](https://doi.org/10.1093/joc/jqy041).
- Peterson, Joshua C. et al. (2019). “Human Uncertainty Makes Classification More Robust”. In: *Proceedings of the IEEE/CVF International Conference on Computer Vision (ICCV)*, pp. 9617–9626.
- Phoenix, Davin L. (2019). *The Anger Gap: How Race Shapes Emotion in Politics*. Cambridge University Press.

- Plank, Barbara (2022). “The “Problem” of Human Label Variation: On Ground Truth in Data, Modeling and Evaluation”. In: *Proceedings of EMNLP 2022*. Abu Dhabi: ACL.
- Prabhakaran, Vinodkumar, Aida Mostafazadeh Davani, and Mark Diaz (2021). “On Releasing Annotator-Level Labels and Information in Datasets”. In: *Proceedings of the Joint 15th Linguistic Annotation Workshop (LAW) and 3rd DMR Workshop*. Punta Cana: ACL, pp. 133–138.
- Prior, Markus (2007). *Post-Broadcast Democracy: How Media Choice Increases Inequality in Political Involvement and Polarizes Elections*. Cambridge: Cambridge University Press.
- Radford, Alec et al. (2021). “Learning Transferable Visual Models From Natural Language Supervision”. In: *Proceedings of the 38th International Conference on Machine Learning (ICML)*. PMLR 139, pp. 8748–8763.
- Raykar, Vikas C. et al. (2010). “Learning from Crowds”. In: *Journal of Machine Learning Research* 11, pp. 1297–1322.
- Reny, Tyler T., Loren Collingwood, and Ali A. Valenzuela (2019). “Vote Switching in the 2016 Election: How Racial and Immigration Attitudes, Not Economics, Explain Shifts in White Voting”. In: *Public Opinion Quarterly* 83.1, pp. 91–113.
- Rodden, Jonathan A. (2019). *Why Cities Lose: The Deep Roots of the Urban–Rural Political Divide*. New York: Basic Books.
- Rodrigues, Filipe and Francisco C. Pereira (2018). “Deep Learning from Crowds”. In: *Proceedings of the 32nd AAAI Conference on Artificial Intelligence*, pp. 1611–1618. DOI: [10.1609/aaai.v32i1.11506](https://doi.org/10.1609/aaai.v32i1.11506).
- Röttger, Paul et al. (2022). “Two Contrasting Data Annotation Paradigms for Subjective NLP Tasks”. In: *Proceedings of the 2022 Conference of the North American Chapter of the Association for Computational Linguistics: Human Language Technologies*. ACL, pp. 175–190. DOI: [10.18653/v1/2022.naacl-main.13](https://doi.org/10.18653/v1/2022.naacl-main.13).

- Russell, Bryan C. et al. (2008). "LabelMe: A Database and Web-Based Tool for Image Annotation". In: *International Journal of Computer Vision* 77.1–3, pp. 157–173. DOI: [10.1007/s11263-007-0090-8](https://doi.org/10.1007/s11263-007-0090-8).
- Santurkar, Shibani et al. (2023). "Whose Opinions Do Language Models Reflect?" In: *Proceedings of the 40th International Conference on Machine Learning (ICML)*.
- Sap, Maarten, Dallas Card, et al. (2019). "The Risk of Racial Bias in Hate Speech Detection". In: *Proceedings of the 57th Annual Meeting of the ACL*. Florence, Italy, pp. 1668–1678. DOI: [10.18653/v1/P19-1163](https://doi.org/10.18653/v1/P19-1163).
- Sap, Maarten, Swabha Swayamdipta, et al. (2022). "Annotators with Attitudes: How Annotator Beliefs and Identities Bias Toxic Language Detection". In: *Proceedings of NAACL-HLT 2022*, pp. 5884–5906. DOI: [10.18653/v1/2022.naacl-main.431](https://doi.org/10.18653/v1/2022.naacl-main.431).
- Schaekermann, Mike et al. (2018). "Resolvable vs. Irresolvable Disagreement: A Study on Worker Deliberation in Crowd Work". In: *Proceedings of the ACM on Human-Computer Interaction*. Vol. 2. CSCW. CSCW Best Paper Award, Article 154, 1–19. DOI: [10.1145/3274423](https://doi.org/10.1145/3274423).
- Schaffner, Brian F., Matthew MacWilliams, and Tatishe Nteta (2018). "Understanding White Polarization in the 2016 Vote for President: The Sobering Role of Racism and Sexism". In: *Political Science Quarterly* 133.1, pp. 9–34.
- Schattschneider, E. E. (1960). *The Semi-Sovereign People: A Realist's View of Democracy in America*. New York: Holt, Rinehart and Winston.
- Schmitt, Carl (2007). *The Concept of the Political: Expanded Edition*. Originally published 1932. Translated by George Schwab. University of Chicago Press.
- Sides, John, Michael Tesler, and Lynn Vavreck (2018). *Identity Crisis: The 2016 Presidential Campaign and the Battle for the Meaning of America*. Princeton University Press.
- Sobolev, Anton et al. (2020). "News and Geolocated Social Media Accurately Measure Protest Size Variation". In: *American Political Science Review* 114.4, pp. 1343–1351.

- Soroka, Stuart et al. (2016). "The Impact of News Photos on Support for Military Action". In: *Political Communication* 33.4, pp. 563–582. DOI: [10.1080/10584609.2015.1133745](https://doi.org/10.1080/10584609.2015.1133745).
- Steinert-Threlkeld, Zachary C., Alexander Chan, and Jungseock Joo (2022). "How State and Protester Violence Affect Protest Dynamics". In: *Journal of Politics* 84.2, pp. 798–813.
- Tajfel, Henri and John C. Turner (1979). "An Integrative Theory of Intergroup Conflict". In: *The Social Psychology of Intergroup Relations*. Ed. by William G. Austin and Stephen Worchel. Monterey, CA: Brooks/Cole, pp. 33–47.
- Todorov, Alexander (2017). *Face Value: The Irresistible Influence of First Impressions*. Princeton University Press.
- Todorov, Alexander et al. (2005). "Inferences of Competence from Faces Predict Election Outcomes". In: *Science* 308.5728, pp. 1623–1626.
- Torres, Michelle (2021). "Framing a Protest: Determinants and Effects of Visual Frames". Working paper.
- Torres, Michelle and Francisco Cantú (2022). "Learning to See: Convolutional Neural Networks for the Analysis of Social Science Data". In: *Political Analysis* 30.1, pp. 113–131.
- Uma, Alexandra N. et al. (2021). "Learning from Disagreement: A Survey". In: *Journal of Artificial Intelligence Research* 72, pp. 1385–1470. DOI: [10.1613/jair.1.12752](https://doi.org/10.1613/jair.1.12752).
- Waseem, Zeerak (2016). "Are You a Racist or Am I Seeing Things? Annotator Influence on Hate Speech Detection on Twitter". In: *Proceedings of the First Workshop on NLP and Computational Social Science*. Austin, TX: ACL, pp. 138–142.
- Webb Williams, Nora, Andreu Casas, Kevin Aslett, et al. (2026). "When Conservatives See Red but Liberals Feel Blue: Labeler Characteristics and Variation in Content Annotation". In: *The Journal of Politics* 88.2, pp. 000–000.
- Webb Williams, Nora, Andreu Casas, and John D. Wilkerson (2020). *Images as Data for Social Science Research: An Introduction to Convolutional Neural Nets for Image Classifi-*

- cation*. Elements in Quantitative and Computational Methods for the Social Sciences. Cambridge University Press. DOI: [10.1017/9781108860741](https://doi.org/10.1017/9781108860741).
- Won, Donghyeon, Zachary C Steinert-Threlkeld, and Jungseock Joo (2017). “Protest Activity Detection and Perceived Violence Estimation from Social Media Images”. In: *Proceedings of the 25th ACM International Conference on Multimedia*, pp. 786–794.
- Wright, Erik Olin (1997). *Class Counts: Comparative Studies in Class Analysis*. Cambridge University Press.
- Xi, Nan et al. (2020). “Understanding the Political Ideology of Legislators from Social Media Images”. In: *Proceedings of the 14th International AAAI Conference on Web and Social Media (ICWSM)*. Vol. 14, pp. 726–737.
- Xu, Yuxiang and David Jurgens (2026). *Beyond Consensus: Perspectivist Modeling and Evaluation of Annotator Disagreement in NLP*. Cited as 2025 in manuscript; arXiv version dated January 2026. arXiv: [2601.09065](https://arxiv.org/abs/2601.09065).
- Yang, JungHwan, Richard A. Davis, and Matthew Hindman (2023). “Visual Misinformation on Facebook”. In: *Journal of Communication* 73.4, pp. 316–328.
- Yarkoni, Tal and Jacob Westfall (2017). “Choosing Prediction Over Explanation in Psychology: Lessons From Machine Learning”. In: *Perspectives on Psychological Science* 12.6, pp. 1100–1122.
- Yarowsky, David (1995). “Unsupervised Word Sense Disambiguation Rivaling Supervised Methods”. In: *Proceedings of the 33rd ACL*, pp. 189–196. DOI: [10.3115/981658.981684](https://doi.org/10.3115/981658.981684).

Appendix

A Full Classification Results

This appendix presents the complete classification results for all axes tested and explains the accuracy threshold used to determine which axes produce reliable classifiers. Political and cross-political axes use the main PVPS classifier (Figure 2). Sociodemographic axes (within-party, within-ideology, within-thermometer, and standalone social) use the extended pipeline (Figure 4).

A.1 What counts as a working classifier?

A classifier is useful when it predicts the correct label substantially more often than a coin flip. For a binary task, chance accuracy is 50%. I set the working threshold at 65%, fifteen percentage points above chance, for three reasons.

First, the prediction target differs from standard image classification. The classifier does not identify objects in an image; it predicts which of two political or social location groups rated the image more positively. Each image in the main survey was rated by approximately 65 respondents on average, producing unusually rich ground-truth labels. Most computational work on political images relies on a single annotator or a small crowd panel per item (Casas and Webb Williams, 2019; Won et al., 2017); the present study aggregates dozens of ratings per image, which yields more precise estimates of group-level evaluative differences. Comparable studies that predict political orientation from visual data report accuracies in the 70–75% range even with far larger training sets. Kosinski (2021) achieve 72% from over one million facial photographs, and Won et al. (2017) report AUC $\sim .97$ for protest detection from 40,764 images, a less subjective target than evaluative divergence. The present study works with 1,264 primary images and a more abstract prediction target than object recognition, making 65% a conservative threshold.

This threshold applies to the minimum per-class accuracy, the accuracy on whichever class is harder to predict. Overall accuracy on passing axes is higher in every case.

Second, the training set is compact by machine learning standards. Each of the 100 training runs (10 seeds \times 10 ensemble members) uses roughly 1,075 images for training and 189 for testing. Intersectional axes (for example, Female Democrats versus Male Republicans) further reduce the usable sample to 200–400 images. That the classifier achieves 65–83% accuracy in this regime, without pretraining on millions of labeled examples, suggests that the evaluative signal in political images is strong enough to be captured even from limited data.

Third, the classifier is a measurement tool and apparently not the only decision system. When it is later applied to label new, unseen images, any systematic errors can be corrected statistically using the approach proposed by Egami et al. (2024). What matters is that accuracy is reliably above chance, stable across the 10 runs, and not achieved by always guessing the larger class.³²

A.2 How to read Table 5

Each row is one classification axis. The columns report the following.

- **Grp A, Grp B** give the classifier’s accuracy on each of the two groups separately. For example, in the row “Female Dem vs Male Rep,” Grp A is the share of Female-Democrat-preferred images correctly identified, and Grp B is the share of Male-Republican-preferred images correctly identified. If either number is near 50%, the classifier cannot reliably distinguish that group’s images from the other’s.

³²A classifier that predicts “consensus” for every image in a dataset where 60% of images are consensus would reach 60% accuracy but would be useless. Per-class accuracy, reported separately for each group, guards against this.

Table 5: Classification results for all axes. Grp A and Grp B give per-class accuracy (%) for the first and second group named in each axis. * = both groups above 75%; • = both above 65%; ○ = min-class $\geq 60\%$ (Stack V2 axes only). All values are medians across 10 seeds. DemL = Dem-leaning (feeling thermometer); RepL = Rep-leaning. Political and cross-political axes use the main PVPS classifier. Sociodemographic axes (marked Stack V2) use the extended pipeline.

Axis	Grp A (%)	Grp B (%)	
<i>Primary political axes</i>			
IDEOLOGY	81.6	78.9	*
THERMOMETER	79.8	78.5	*
PARTY	68.7	69.6	•
<i>Social axes, no partisan conditioning (Stack V2)</i>			
AGE	70.5	68.9	•
GENDER	67.4	62.0	○
EDUCATION	65.3	61.0	○
HISPANIC	63.8	57.5	
INCOME	63.3	53.5	
<i>Cross-party</i>			
Female Dem vs Male Rep	79.4	75.5	*
HighInc Dem vs LowInc Rep	81.8	81.6	*
Hisp Dem vs NonHisp Rep	78.1	83.8	*
LowInc Dem vs HighInc Rep	83.6	79.3	*
Young Dem vs Old Rep	79.5	78.9	*
Liberal Dem vs Conserv Rep	80.9	74.7	•
Strong Dem vs Strong Rep	80.6	74.1	•
HighEdu Dem vs LowEdu Rep	82.6	73.5	•
Old Dem vs Young Rep	82.5	73.1	•
Male Dem vs Female Rep	83.2	70.5	•

Continued on next page

Table 5 continued

Axis	Grp A (%)	Grp B (%)	
LowEdu Dem vs HighEdu Rep	78.3	67.7	•
NonHispanic Dem vs Hispanic Rep	73.7	60.0	
Moderate Dem vs Moderate Rep	57.1	54.5	
WeakDem vs WeakRep	54.0	63.5	
<i>Cross-ideology</i>			
HighEdu Lib vs LowEdu Con	86.5	80.4	*
Male Lib vs Female Con	82.9	75.0	*
Old Lib vs Young Con	77.4	74.5	•
DemLean Lib vs RepLean Con	80.7	74.6	•
LowInc Lib vs HighInc Con	78.9	71.7	•
Female Lib vs Male Con	83.5	72.0	•
LowEdu Lib vs HighEdu Con	75.0	76.8	*
Young Lib vs Old Con	76.6	77.6	*
HighInc Lib vs LowInc Con	77.3	72.7	•
Hispanic Lib vs NonHispanic Con	76.1	64.7	
NonHispanic Lib vs Hispanic Con	71.8	62.8	
RepLean Lib vs DemLean Con	45.5	44.4	
<i>Cross-thermometer</i>			
HighEdu DemL vs LowEdu RepL	81.3	78.8	*
LowEdu DemL vs HighEdu RepL	78.1	76.9	*
Young DemL vs Old RepL	77.3	82.8	*
Female DemL vs Male RepL	80.0	75.0	*
Male DemL vs Female RepL	81.7	75.0	*
LowInc DemL vs HighInc RepL	79.5	75.0	*
HighInc DemL vs LowInc RepL	81.6	70.2	•

Continued on next page

Table 5 continued

Axis	Grp A (%)	Grp B (%)	
Hispanic DemL vs NonHispanic RepL	82.3	70.4	•
Old DemL vs Young RepL	80.7	68.3	•
NonHispanic DemL vs Hispanic RepL	63.9	57.1	
<i>Same-sociodemographic, cross-party</i>			
Female Dem vs Female Rep	82.1	82.0	*
HighEdu Dem vs HighEdu Rep	80.6	77.2	*
LowEdu Dem vs LowEdu Rep	79.2	73.2	•
Young Dem vs Young Rep	76.1	71.7	•
LowInc Dem vs LowInc Rep	77.0	71.4	•
NonHispanic Dem vs NonHispanic Rep	84.2	71.1	•
HighInc Dem vs HighInc Rep	80.9	71.6	•
Male Dem vs Male Rep	83.3	70.6	•
Old Dem vs Old Rep	81.5	69.2	•
Hispanic Dem vs Hispanic Rep	54.2	59.0	
<i>Same-sociodemographic, cross-ideology</i>			
Old Lib vs Old Con	86.2	79.7	*
HighEdu Lib vs HighEdu Con	79.6	80.0	*
Female Lib vs Female Con	81.0	76.9	*
NonHispanic Lib vs NonHispanic Con	84.4	75.0	*
Male Lib vs Male Con	83.8	76.2	*
HighInc Lib vs HighInc Con	76.3	73.0	•
LowEdu Lib vs LowEdu Con	76.7	69.8	•
LowInc Lib vs LowInc Con	72.2	72.1	•
Young Lib vs Young Con	70.2	56.5	

Continued on next page

Table 5 continued

Axis	Grp A (%)	Grp B (%)	
Hispanic Lib vs Hispanic Con	60.5	64.4	
<i>Same-sociodemographic, cross-thermometer</i>			
HighEdu DemL vs HighEdu RepL	80.8	77.6	*
Female DemL vs Female RepL	83.6	77.6	*
Old DemL vs Old RepL	82.1	76.8	*
Male DemL vs Male RepL	81.7	74.1	•
LowInc DemL vs LowInc RepL	79.7	73.9	•
LowEdu DemL vs LowEdu RepL	77.8	74.0	•
HighInc DemL vs HighInc RepL	81.2	78.8	*
NonHispanic DemL vs NonHispanic RepL	77.5	71.6	•
Young DemL vs Young RepL	73.0	69.8	•
Hispanic DemL vs Hispanic RepL	45.8	55.9	
<i>Within-party (Stack V2)</i>			
AGE	70.5	68.9	•
Young Rep vs Old Rep	66.7	65.4	•
Young Dem vs Old Dem	65.5	63.6	○
GENDER	67.4	62.0	○
EDUCATION	65.3	61.0	○
HISPANIC	63.8	57.5	
Female Rep vs Male Rep	65.9	57.3	
Female Dem vs Male Dem	58.5	56.8	
HighEdu Dem vs LowEdu Dem	61.7	56.8	
INCOME	63.3	53.5	
Hispanic Dem vs NonHispanic Dem	60.0	53.0	
Hispanic Rep vs NonHispanic Rep	60.0	52.4	

Continued on next page

Table 5 continued

Axis	Grp A (%)	Grp B (%)	
HighEdu Rep vs LowEdu Rep	55.7	51.1	
<i>Within-ideology (Stack V2)</i>			
DemLean Con vs RepLean Con	70.3	64.2	○
Young Con vs Old Con	69.1	63.9	○
Lib DemL vs Con DemL	68.7	63.0	○
Hispanic Con vs NonHispanic Con	62.2	56.4	
Female Con vs Male Con	60.4	56.1	
Young Lib vs Old Lib	56.8	53.4	
HighEdu Lib vs LowEdu Lib	58.3	52.3	
Female Lib vs Male Lib	57.3	51.8	
HighInc Lib vs LowInc Lib	54.1	49.8	
HighInc Con vs LowInc Con	58.0	52.9	
HighEdu Con vs LowEdu Con	50.5	48.0	
Hispanic Lib vs NonHispanic Lib	50.0	42.1	
DemLean Lib vs RepLean Lib	<i>collapsed</i>		
<i>Within-thermometer (Stack V2)</i>			
Young DemL vs Old DemL	63.3	59.5	
Young RepL vs Old RepL	63.0	59.2	
Female RepL vs Male RepL	61.2	55.9	
Female DemL vs Male DemL	57.3	54.5	
HighEdu DemL vs LowEdu DemL	62.1	51.1	
HighEdu RepL vs LowEdu RepL	58.1	50.7	
HighInc DemL vs LowInc DemL	58.1	54.4	
HighInc RepL vs LowInc RepL	57.7	51.6	
Hispanic DemL vs NonHispanic DemL	53.8	46.8	

Continued on next page

Table 5 continued

Axis	Grp A (%)	Grp B (%)
Hispanic RepL vs NonHispanic RepL	55.2	48.7
Liberal RepL vs Conservative RepL	<i>collapsed</i>	

B Calibration and Prediction Stability

Table 6 reports standard classification diagnostics for the three primary political axes.

Table 6: Classification diagnostics for primary political axes. All values are medians across 10 seeds. Accuracy, precision, recall, and F1 are reported as macro-averages (un-weighted mean across the two classes). AUC is the area under the ROC curve.

Axis	Accuracy	Precision	Recall	Macro F1	AUC
PARTY	84.0%	75.4%	82.5%	77.4%	0.874
IDEOLOGY	87.1%	81.9%	83.3%	82.5%	0.906
THERMOMETER	88.7%	85.2%	86.4%	86.4%	0.915

The spread (interquartile range) across 10 seeds is below 4 percentage points on most passing axes, indicating that results are not driven by a lucky train-test split. The primary political axes show spread between 2.4pp (ideology) and 3.8pp (thermometer). Within-group axes that cluster near chance show equally low spread, confirming that these null results are stable, not noisy.

The ensemble’s predicted probabilities for the PARTY axis are bimodal. 69% of test-image predictions fall in the tails (below 0.2 or above 0.9), with 53% of images receiving near-zero probability of class 1 and 14% receiving near-certainty. The classifier is confidently correct on most images, with roughly 20% in the uncertain middle range (0.2–0.8).

C Feature Importance and Ablation

Table 7 reports the ablation study on the PARTY axis (primary data only, 10 seeds per configuration), removing one feature block at a time.

Table 7: Feature ablation on the PARTY axis (primary data only). Each row removes one feature block; other blocks remain. Drop = change from full-model baseline.

Configuration	Median min-acc	Drop
Full model	73.2%	–
– CLIP	70.3%	–2.8pp
– DINOv2	71.3%	–1.9pp
– TF-IDF + Semantic	72.9%	–0.2pp
– Concepts	70.2%	–3.0pp
CLIP only	71.8%	–1.4pp
DINOv2 only	69.8%	–3.3pp

Table 8: Feature ablation on the PARTY axis (primary data only, single-ensemble setup with 10 seeds per row). The full-model baseline of 73.2% reflects this single-ensemble configuration; the corresponding median in the 10-ensemble \times 10-seed configuration used elsewhere in the paper is 68.7% (Table 5). Drop = change from the full-model baseline within this configuration.

Removing concept features (binary indicators of political objects such as protest signs, police, flags, and politicians) produces the largest drop (–3.0pp), followed by CLIP (–2.8pp) and DINOv2 (–1.9pp). Text-based features contribute the least (–0.2pp when TF-IDF captions and semantic word indicators are removed together), suggesting that the partisan signal on this axis is carried by visual content. CLIP alone (71.8%) and DINOv2 alone (69.8%) each approach the full-model baseline without matching it, which means the two pretrained encoders capture complementary aspects of the image. The concept features add information that neither encoder represents on its own, likely because these features were constructed for political image content and encode objects (uniforms, banners, crowd formations) that general-purpose vision models treat as incidental.

The feature vector comprises six blocks totaling 1,666 dimensions. CLIP (512) and DINOv2 (768) are pure visual embeddings extracted from frozen pretrained models. TF-IDF

caption features (300) encode word frequencies in Gemini-generated image descriptions. Semantic word indicators (50) flag the presence of politically predictive terms identified during training. Concept presence features (24) capture high-level scene attributes (see Section G), and political topic features (12) indicate policy-domain relevance.

D Source Prediction Diagnostic

The pipeline includes a pre-training diagnostic that tests whether a simple logistic regression on CLIP and DINOv2 embeddings can distinguish primary-data images from supplementary Webb Williams, Casas, Aslett, et al. (2026) images. If source-classification accuracy exceeds 85%, self-training is disabled automatically.

The diagnostic returns 97.3% accuracy (5 splits, range 96.9–97.4%). The two image pools differ substantially in resolution, framing, and photographic style. For image-level classifiers (the main pipeline of Figure 2 and Path A of the extension), self-training was disabled and the supplementary dataset was excluded from training, since image-level classification could otherwise learn dataset-style differences as spurious signal. Path B of the extension trains on individual (image, respondent) pairs and is fitted on the combined respondent-level pool, which is statistically appropriate because dataset-style differences cannot enter as a per-respondent rule.

E Per-Topic Sociodemographic Classification

When the training data are split by policy topic, sociodemographic axes reveal stable directional patterns that cancel in the aggregate. Table 9 reports per-topic results for each standalone sociodemographic axis. Where 75%+ of images within a topic have the same directional label, the finding is reported as a dominant direction. Where both classes are represented, a classifier is trained on balanced holdout splits (equal class sizes in test,

minimum five per class, ten seeds) and median minimum-class accuracy is reported.

Table 9: Per-topic sociodemographic classification. “Dom.” = dominant direction ($\geq 75\%$ of images have same label). Accuracy = median minimum-class accuracy, 10 seeds, balanced test.

Axis	Immigration	Guns	LGBTQ+	Jan. 6
GENDER	52.3%	Dom. (F, 76%)	Dom. (M, 78%)	22.2%
HISPANIC	Dom. (Hispanic, 76%)	0.0%	Dom. (Hispanic, 82%)	25.0%
AGE	45.2%	14.3%	40.9%	Dom. (Young, 76%)
EDUCATION	51.5%	25.0%	33.3%	Dom. (LowEdu, 82%)
INCOME	43.4%	46.2%	33.3%	41.7%

Where the image-level classifier is tested on balanced holdout sets within a single topic, it performs at or below chance. Gender on immigration reaches 52.3% (966 images, balanced test of 65 per class). Education on immigration reaches 51.5% (906 images). Age on immigration reaches 45.2%. Income falls below chance on every topic. The dominant direction findings confirm that sociodemographic evaluative divergence is real and topic-structured, but the image-level classifier cannot predict from visual content alone which way the demographic gap will go on a specific image.

F Encoder Architecture

Both image encoders (CLIP ViT-B/32 and DINOv2 ViT-B/14) are used as frozen feature extractors. No fine-tuning is performed on any encoder. Images are passed through each pretrained model to obtain fixed-length embedding vectors (512 dimensions from CLIP, 768 from DINOv2), which are L2-normalized and concatenated with the four text and concept feature blocks before being fed to the classification head.

The classification head is a two-block residual network with GELU activations, layer normalization, and dropout. Input is projected to a hidden dimension (128 or 256, selected by cross-validation), passed through two residual blocks, and mapped to class logits. Ten such networks are trained per seed with different random initializations, and

their softmax outputs are averaged to produce the ensemble prediction.

G Concept Feature Definitions

The 24 concept features are binary indicators of political objects and scene attributes. Each feature is set to 1 if the corresponding object or attribute is detected in the Gemini-generated image description, and 0 otherwise. The concepts were drawn from the political image literature (Casas and Webb Williams, 2019; Torres and Cantú, 2022; Won et al., 2017) and refined during development to retain those that contributed to classification accuracy.

The 24 concepts are listed below.

1. American flag
2. Confederate flag
3. Pride rainbow flag
4. Trump sign or hat
5. BLM sign
6. Police
7. Military
8. Protesters
9. Crowd of people
10. Armed people
11. Politicians
12. Guns or weapons
13. Signs or banners
14. Capitol building
15. Church
16. Border wall or fence
17. Violence or conflict
18. Peaceful gathering
19. Voting or election
20. Immigration or migrants
21. Same-sex couple
22. Angry people
23. Happy people
24. Sad or mourning

Each concept is detected by keyword matching against the structured Gemini description (dense description, objects and symbols, political context fields). A concept is coded

1 if any of its trigger keywords appear in the combined text and 0 otherwise.

The 12 political topic features indicate whether the image description contains keywords associated with a policy domain. The 12 domains are climate, economy and labor, education, elections, gender and reproductive rights (covering MeToo, women’s march, abortion, Roe v. Wade, Planned Parenthood, reproductive rights, and Kavanaugh hearings as a single dimension), guns, healthcare, immigration, LGBTQ+, military and foreign policy, race and policing, and Trump administration. These features help the classifier differentiate images from distinct policy contexts. Wave 4 includes January 6 imagery (see Table 3); these images do not have a dedicated topic-feature dimension and instead activate the closest semantically related dimensions (Trump administration, race and policing, or elections) depending on caption content.

H Full Evaluative Profiles

Figures 7 display the complete evaluative profiles across all axes for three held-out test images (military at border, LGBTQ+ rally, January 6). Black bold triangles mark predictions from the main classifier (holdout accuracy $\geq 65\%$, applicable to any image). Blue bold triangles mark predictions from the extended sociodemographic pipeline (Stack V2, median min-class accuracy $\geq 60\%$). Gray rows indicate axes that do not reach either threshold for the given image.

Figure 7: Full evaluative profiles



STANDALONE POLITICAL

Party	▲ Dem.	Rep.	97%	▲ Dem.	Rep.	97%	Dem.	▲ Rep.	95%
Ideology	▲ Lib.	Con.	98%	▲ Lib.	Con.	97%	Lib.	▲ Con.	97%
Therm.	▲ Dem-lean.	Rep-lean.	96%	▲ Dem-lean.	Rep-lean.	95%	Dem-lean.	▲ Rep-lean.	94%

STANDALONE SOCIAL

Age	▲ Young	Old		Young	▲ Old		▲ Young	Old	
Gender	▲ Female	Male		Female	Male		▲ Female	Male	
Education	▲ LowEdu	HighEdu		LowEdu	▲ HighEdu		▲ LowEdu	HighEdu	

CROSS-PARTY (SOCIODEM. x PARTY)

Age*Pty	▲ Young Dem.	Old Rep.	86%	▲ Young Dem.	Old Rep.	91%	Young Dem.	▲ Old Rep.	72%
Age*Pty	▲ Old Dem.	Young Rep.	91%	▲ Old Dem.	Young Rep.	93%	Old Dem.	▲ Young Rep.	82%
Gen.*Pty	▲ Fem. Dem.	Male Rep.	89%	▲ Fem. Dem.	Male Rep.	89%	Fem. Dem.	▲ Male Rep.	79%
Gen.*Pty	▲ Male Dem.	Fem. Rep.	93%	▲ Male Dem.	Fem. Rep.	97%	Male Dem.	▲ Fem. Rep.	90%
Edu.*Pty	▲ HiEd Dem.	LowEd Rep.	92%	▲ HiEd Dem.	LowEd Rep.	88%	HiEd Dem.	▲ LowEd Rep.	86%
Edu.*Pty	▲ LowEd Dem.	HiEd Rep.	82%	▲ LowEd Dem.	HiEd Rep.	88%	LowEd Dem.	▲ HiEd Rep.	70%
Inc.*Pty	▲ HiInc Dem.	LoInc Rep.	93%	▲ HiInc Dem.	LoInc Rep.	85%	HiInc Dem.	▲ LoInc Rep.	94%
Inc.*Pty	▲ LoInc Dem.	HiInc Rep.	98%	▲ LoInc Dem.	HiInc Rep.	98%	LoInc Dem.	▲ HiInc Rep.	90%
Hisp.*Pty	▲ Hisp Dem.	NonH Rep.	79%	▲ Hisp Dem.	NonH Rep.	78%	Hisp Dem.	▲ NonH Rep.	69%
Str.*Pty	▲ Strong Dem.	Strong Rep.	97%	▲ Strong Dem.	Strong Rep.	96%	Strong Dem.	▲ Strong Rep.	94%
Thm*Pty	▲ Cool Rep.	Warm Rep.	55%	▲ Cool Rep.	Warm Rep.	69%	▲ Cool Rep.	Warm Rep.	57%
Ideo*Pty	▲ Lib. Dem.	Con. Rep.	97%	▲ Lib. Dem.	Con. Rep.	97%	Lib. Dem.	▲ Con. Rep.	94%

▲ = group predicted to evaluate this image more positively.
 Black = classifier (holdout >= 65%). Gray = below threshold. Numbers = confidence %.

Military at Border

LGBTQ+ Rally

January 6

CROSS-IDEOLOGY (SOCIODEM. x IDEO.)

Age*Ideo	▲ Young Lib.	Old Con.	95%	▲ Young Lib.	Old Con.	95%	Young Lib.	▲ Old Con.	92%
Age*Ideo	▲ Old Lib.	Young Con.	90%	▲ Old Lib.	Young Con.	90%	Old Lib.	▲ Young Con.	88%
Gen.*Ideo	▲ Fem. Lib.	Male Con.	88%	▲ Fem. Lib.	Male Con.	89%	Fem. Lib.	▲ Male Con.	89%
Gen.*Ideo	▲ Male Lib.	Fem. Con.	91%	▲ Male Lib.	Fem. Con.	93%	Male Lib.	▲ Fem. Con.	78%
Edu.*Ideo	▲ HiEd Lib.	LowEd Con.	92%	▲ HiEd Lib.	LowEd Con.	90%	HiEd Lib.	▲ LowEd Con.	94%
Edu.*Ideo	LowEd Lib.	HiEd Con.		LowEd Lib.	HiEd Con.		LowEd Lib.	HiEd Con.	
Inc.*Ideo	▲ HiInc Lib.	LoInc Con.	87%	▲ HiInc Lib.	LoInc Con.	87%	HiInc Lib.	▲ LoInc Con.	86%
Inc.*Ideo	▲ LoInc Lib.	HiInc Con.	96%	▲ LoInc Lib.	HiInc Con.	97%	LoInc Lib.	▲ HiInc Con.	96%
Lean*Ideo	▲ DemL Lib.	RepL Con.	97%	▲ DemL Lib.	RepL Con.	98%	DemL Lib.	▲ RepL Con.	97%

CROSS-THERMOMETER (SOCIODEM. x THERM.)

Age*Thm	▲ Young DemL.	Old RepL.	93%	▲ Young DemL.	Old RepL.	83%	Young DemL.	▲ Old RepL.	67%
Age*Thm	▲ Old DemL.	Young RepL.	77%	▲ Old DemL.	Young RepL.	81%	Old DemL.	▲ Young RepL.	85%
Gen.*Thm	▲ Fem. DemL.	Male RepL.	86%	▲ Fem. DemL.	Male RepL.	91%	Fem. DemL.	▲ Male RepL.	90%
Gen.*Thm	▲ Male DemL.	Fem. RepL.	96%	▲ Male DemL.	Fem. RepL.	95%	Male DemL.	▲ Fem. RepL.	89%
Edu.*Thm	▲ HiEd DemL.	LowEd RepL.	96%	▲ HiEd DemL.	LowEd RepL.	94%	HiEd DemL.	▲ LowEd RepL.	94%
Edu.*Thm	LowEd DemL.	HiEd RepL.		LowEd DemL.	HiEd RepL.		LowEd DemL.	HiEd RepL.	
Inc.*Thm	▲ HiInc DemL.	LoInc RepL.	90%	▲ HiInc DemL.	LoInc RepL.	85%	HiInc DemL.	▲ LoInc RepL.	87%
Inc.*Thm	▲ LoInc DemL.	HiInc RepL.	96%	▲ LoInc DemL.	HiInc RepL.	97%	LoInc DemL.	▲ HiInc RepL.	80%
Hisp.*Thm	▲ Hisp DemL.	NonH RepL.	88%	▲ Hisp DemL.	NonH RepL.	79%	Hisp DemL.	▲ NonH RepL.	82%

▲ = group predicted to evaluate this image more positively.
 Black = classifier (holdout >= 65%). Gray = below threshold. Numbers = confidence %.

Military at Border
SAME-SOCDEM, CROSS-PARTY

LGBTQ+ Rally

January 6

Female	▲ Fem. Dem.	Fem. Rep.	96%	▲ Fem. Dem.	Fem. Rep.	97%	▲ Fem. Dem.	Fem. Rep.	77%
Male	▲ Male Dem.	Male Rep.	88%	▲ Male Dem.	Male Rep.	93%	Male Dem.	▲ Male Rep.	84%
Young	Young Dem.	Young Rep.		Young Dem.	Young Rep.		Young Dem.	Young Rep.	
Old	▲ Old Dem.	Old Rep.	97%	▲ Old Dem.	Old Rep.	96%	Old Dem.	▲ Old Rep.	92%
HiEd	▲ HiEd Dem.	HiEd Rep.	99%	▲ HiEd Dem.	HiEd Rep.	99%	HiEd Dem.	▲ HiEd Rep.	97%
LowEd	▲ LowEd Dem.	LowEd Rep.	85%	▲ LowEd Dem.	LowEd Rep.	90%	LowEd Dem.	▲ LowEd Rep.	70%
NonH	▲ NonH Dem.	NonH Rep.	96%	▲ NonH Dem.	NonH Rep.	96%	NonH Dem.	▲ NonH Rep.	96%
HiInc	▲ HiInc Dem.	HiInc Rep.	97%	▲ HiInc Dem.	HiInc Rep.	96%	HiInc Dem.	▲ HiInc Rep.	95%
LoInc	▲ LoInc Dem.	LoInc Rep.	95%	▲ LoInc Dem.	LoInc Rep.	96%	LoInc Dem.	▲ LoInc Rep.	89%

SAME-SOCDEM, CROSS-IDEOLOGY

Female	▲ Fem. Lib.	Fem. Con.	96%	▲ Fem. Lib.	Fem. Con.	96%	Fem. Lib.	▲ Fem. Con.	85%
Male	▲ Male Lib.	Male Con.	97%	▲ Male Lib.	Male Con.	97%	Male Lib.	▲ Male Con.	91%
Old	▲ Old Lib.	Old Con.	98%	▲ Old Lib.	Old Con.	97%	Old Lib.	▲ Old Con.	96%
HiEd	▲ HiEd Lib.	HiEd Con.	97%	▲ HiEd Lib.	HiEd Con.	97%	HiEd Lib.	▲ HiEd Con.	96%
LowEd	LowEd Lib.	LowEd Con.		LowEd Lib.	LowEd Con.		LowEd Lib.	LowEd Con.	
NonH	▲ NonH Lib.	NonH Con.	97%	▲ NonH Lib.	NonH Con.	96%	NonH Lib.	▲ NonH Con.	96%
HiInc	▲ HiInc Lib.	HiInc Con.	95%	▲ HiInc Lib.	HiInc Con.	94%	HiInc Lib.	▲ HiInc Con.	92%
LoInc	▲ LoInc Lib.	LoInc Con.	94%	▲ LoInc Lib.	LoInc Con.	94%	LoInc Lib.	▲ LoInc Con.	90%

▲ = group predicted to evaluate this image more positively.
 Black = classifier (holdout >= 65%). Gray = below threshold. Numbers = confidence %.

Military at Border

LGBTQ+ Rally

January 6

SAME-SOCDEM, CROSS-THERMOMETER

Female	▲ Fem. DemL.	Fem. RepL.	93%	▲ Fem. DemL.	Fem. RepL.	95%	Fem. DemL.	▲ Fem. RepL.	73%
Male	▲ Male DemL.	Male RepL.	93%	▲ Male DemL.	Male RepL.	89%	Male DemL.	▲ Male RepL.	92%
Young	Young DemL.	Young RepL.		Young DemL.	Young RepL.		Young DemL.	Young RepL.	
Old	▲ Old DemL.	Old RepL.	96%	▲ Old DemL.	Old RepL.	96%	Old DemL.	▲ Old RepL.	96%
HiEd	▲ HiEd DemL.	HiEd RepL.	98%	▲ HiEd DemL.	HiEd RepL.	97%	HiEd DemL.	▲ HiEd RepL.	96%
LowEd	LowEd DemL.	LowEd RepL.		LowEd DemL.	LowEd RepL.		LowEd DemL.	LowEd RepL.	
NonH	▲ NonH DemL.	NonH RepL.	97%	▲ NonH DemL.	NonH RepL.	96%	NonH DemL.	▲ NonH RepL.	95%
HiInc	▲ HiInc DemL.	HiInc RepL.	97%	▲ HiInc DemL.	HiInc RepL.	96%	HiInc DemL.	▲ HiInc RepL.	95%
LoInc	▲ LoInc DemL.	LoInc RepL.	96%	▲ LoInc DemL.	LoInc RepL.	95%	LoInc DemL.	▲ LoInc RepL.	92%

WITHIN-PARTY (SOCIODEM. | PARTY)

Age Dem	▲ Young Dem.	Old Dem.		Young Dem.	▲ Old Dem.		Young Dem.	Old Dem.	
Age Rep	Young Rep.	▲ Old Rep.		Young Rep.	Old Rep.		Young Rep.	▲ Old Rep.	

WITHIN-IDEOLOGY (SOCIODEM. | IDEO.)

Age Con	Young Con.	▲ Old Con.		▲ Young Con.	Old Con.		▲ Young Con.	Old Con.	
Lean Con	DemL Con.	▲ RepL Con.		DemL Con.	▲ RepL Con.		DemL Con.	▲ RepL Con.	
Ideo DemL	Lib. DemL.	▲ Con. DemL.		Lib. DemL.	▲ Con. DemL.		Lib. DemL.	Con. DemL.	

TOPIC-SPECIFIC SOCIODEM. (per-topic dominant direction)

Gender	Female	Male		Female	▲ Male	78%	Female	Male	
Hispanic	▲ Hispanic	NonHisp.	76%	▲ Hispanic	NonHisp.	82%	Hispanic	NonHisp.	
Age	Young	Old		Young	Old		▲ Young	Old	76%
Education	LowEdu	HighEdu		LowEdu	HighEdu		▲ LowEdu	HighEdu	82%

▲ = group predicted to evaluate this image more positively.
 Black = classifier (holdout >= 65%). Gray = below threshold. Numbers = confidence %.

I Summary of Passing Axes

Table 10: Summary of axes by category. Political axes use the main PVPS classifier (Figure 2); the 65% threshold applies. Sociodemographic axes use the extended pipeline (Figure 4); the 60% threshold applies. Pass = median min-class accuracy above the relevant threshold.

Category	Threshold	Pass / Total	Pass rate
Primary political	65%	3 / 3	100%
Cross-party	65%	11 / 14	79%
Cross-ideology	65%	9 / 12	75%
Cross-thermometer	65%	9 / 10	90%
Same-socdem, cross-party	65%	9 / 10	90%
Same-socdem, cross-ideology	65%	8 / 10	80%
Same-socdem, cross-thermometer	65%	9 / 10	90%
Within-party (Stack V2)	60%	5 / 13	38%
Within-ideology (Stack V2)	60%	3 / 12	25%
Within-thermometer (Stack V2)	60%	0 / 11	0%
Standalone social (Stack V2)	60%	3 / 5	60%